

Revue des Composites et des Matériaux Avancés-Journal of Composite and Advanced Materials

Vol. 35, No. 5, October, 2025, pp. 803-821

Journal homepage: http://iieta.org/journals/rcma

Synergistic Impact of Supplementary Cementitious Materials and Steel Fiber on the Performance of Treated Recycled Aggregate Concrete



Bassam Sulaiman Dabbour^{1,2}, Mohd Zulham Affandi Bin Mohd Zahid^{1*}, Badorul Hisham Bin Abu Bakar¹, Noorhazlinda Binti Abd Rahman¹, Abrahem Ahsin Blash^{1,3}

- ¹ School of Civil Engineering, Engineering Campus, Universiti Sains Malaysia, Pulau Pinang 14300, Malaysia
- ² Department of Engineering Sciences and Applied Arts, University College of Science and Technology- Khan Yunis, Gaza Strip P930, Palestine
- ³ Department of Civil Engineering, College of Engineering Technology Houn, Houn 61160, Libya

Corresponding Author Email: mohdzulham@usm.my

Copyright: ©2025 The authors. This article is published by IIETA and is licensed under the CC BY 4.0 license (http://creativecommons.org/licenses/by/4.0/).

https://doi.org/10.18280/rcma.350502

Received: 13 August 2025 Revised: 13 September 2025 Accepted: 9 October 2025

Available online: 31 October 2025

Keywords:

TRAC, SCMs, rapid chloride permeability, impact energy

ABSTRACT

Utilizing recycled aggregates (RA) from concrete waste offers a sustainable solution. However, recycled aggregate concrete (RAC) often exhibits limitations in strength and durability, restricting its broader application. This study evaluates methods to enhance the performance of RAC by treating RA with 0.1M HCl, using a two-stage mixing approach (TSMA), incorporating 0.5% steel fiber (STF), and adding one or two supplementary cementitious materials (SCMs). The SCMs include 10% silica fume (SF), 15% fly ash (FA), and 5% kaolin (KA), used individually or in combination. Significant improvements were observed in the mechanical and durability properties of treated recycled aggregate concrete (TRAC). For instance, the R7-STF0.5-SF10-FA15 mix exhibited a 28.92% increase in compressive strength, a 38.62% rise in splitting tensile strength, and a 40.80% enhancement in flexural strength compared to the reference concrete mix. Flexural toughness and stiffness improved by 333.50% and 131.19%, respectively, while flexural impact energy increased by 499.39% at the initial crack and 600.49% at failure. Durability metrics also showed significant improvements, with reductions in absorption (38.20%), water permeability (81.50%), and rapid chloride permeability (84.40%). The combination of TRA, TSMA, 0.5% STF, and SCMs substantially improves TRAC properties, surpassing those of conventional concrete in strength, durability, ductility, and resistance to dynamic loads.

1. INTRODUCTION

Rapid urbanization and population growth have accelerated the replacement of outdated or unsuitable buildings with modern structures designed to meet increasing housing demands and support societal development. This process generates substantial quantities of concrete rubble from demolition activities [1]. China generates an annual amount of 200 million tons of building rubble through demolishing existing old buildings, in addition to the waste from reconstruction [2]. In contrast, Australia produces 43.78 million tons of waste every year, with 38% of that waste originating from the construction and demolition of buildings [2] Inadequate management of concrete rubble or failure to reuse it in beneficial projects can lead to environmental and economic complications. The best uses for concrete rubble are as RA in concrete building projects or as a subgrade material in road construction [3]. The decomposition of concrete debris when placed in soil or an open area can span several decades, creating a conducive environment for the proliferation of harmful insects and animals that can transmit dangerous diseases [4].

If concrete rubble is not used as RA in concrete, it would lead to the depletion of natural resources, specifically natural aggregate (NA). Moreover, its economic benefit would be wasted [5]. RA exhibits inferior quality compared to NA because of the presence of adhering mortar on the aggregate. Therefore, the specific gravity of RA decreases while its absorption percentage increases compared to NA. The specific gravity of RA mostly ranged from 2.2 to 2.7, whereas for NA, it ranged from 2.5 to 2.85. The absorption percentage of RA usually ranged from 4.5% to 7.0%, whereas for NA, it ranged from 0.4% to 2% [6, 7].

Various studies have investigated the utilization of RA as a replacement for NA, either partially or fully. However, the findings of these studies indicate that the mechanical properties of recycled aggregate concrete (RAC) are inferior to those of normal aggregate concrete (NAC), resulting in reduced strength and durability. As the percentage of RA increases, the compressive, splitting, and flexural strength will decrease, and the absorption, rapid chloride permeability, and water permeability will increase [8, 9]. Several studies have

investigated the effects of total replacing NA with RA on the properties of concrete, where Bai et al. [10] observed that the complete replacement of NA with RA resulted in a reduction of 19%, 15%, and 11% in compressive, splitting, and flexural strength, respectively, compared to NAC. Joseph et al. [11] found that the compressive, splitting, and flexural strength decreased by 19%, 19%, and 4% when the NA was replaced with 60% RA. Several studies have shown that replacing NA with RA results in reduced compressive strength and splitting strength, with decreases ranging from 12% to 47% in compressive strength and from 15% to 39% in splitting strength [11, 12]. Wang et al. [7] conducted a comprehensive analysis of multiple prior studies to examine the impact of replacing NA with RA. Researchers discovered that when the replacement was complete, the average decrease in compressive strength across 37 tests was 14%. Additionally, the reduction in splitting strength was 16%, while the decrease in flexural strength was 11%.

The mechanical properties of RAC can be improved by treating the RA to remove the weak mortar or by strengthening the surface. This treatment can be carried out using various methods, including mechanical rubbing, grinding in a Los Angeles machine, washing with water, chemical treatment, heat treatment, and carbonation treatment [13, 14]. A prominent surface-coating technique for enhancing the properties of RA is the application of a silica fume slurry. This process seals surface micro-cracks and pores, improving the aggregate's density and reducing its water absorption [6].

Although techniques such as mechanical rubbing and grinding with a Los Angeles abrasion machine show negligible environmental impact at the laboratory scale, their large-scale application is hindered by the requirement for heavy machinery, considerable energy consumption, and elevated operational costs. Therefore, the sustainability of these treatments requires careful evaluation, as the associated environmental and economic drawbacks may surpass the potential performance improvements when applied outside controlled experimental settings.

Previous studies have shown that using hydrochloric acid (HCL) to treat RA results in a decrease in absorption, an increase in specific gravity, and a reduction in abrasion. The absorption decreases by 4% to 26%, specific gravity increases by 0.4% to 3.0%, and abrasion decreases by 20% to 26% [15-17]. When sulfuric acid (H₂SO₄) is used to treat RA, the absorption decreases by 29% to 48%, the specific gravity increases by 7% to 8%, and the abrasion reduces by 26% to 30% [16, 18]. However, utilizing nitric acid (HNO₃) results in a 25 to 29% reduction in absorption, a 3.24% to 3.2% increase in specific gravity, and a decrease in abrasion ranging from 26.3% to 2.3% [17]. The utilization of mechanical rubbing in the treatment of RA led to a reduction in absorption by 32% to 41%, an enhancement in specific gravity by 3.5% to 4.6%, and a decrease in abrasion by 34% to 40% [19, 20]. In this study, the RA was treated using hydrochloric acid with a concentration of 0.1M. This treatment method yielded satisfactory results and facilitated the disposal of the remaining solution once the treatment process was completed.

An additional method to enhance concrete properties is by incorporating SCMs such as densified silica fume (SF), fly ash (FA), and kaolin (KA). These materials can improve various mechanical properties, including strength, and significantly enhance the concrete's durability, reducing absorption, rapid chloride permeability, and water permeability [21-23]. SCMs, such as SF, FA, and KA, contain substantial quantities of

silicon dioxide (SiO₂), often known as silica. For example, SF, FA, and KA generally have SiO₂ percentages that fall within the ranges of 80% to 99%, 60% to 75%, and 40% to 50%, respectively [24, 25]. The SiO₂ reacts chemically with the calcium hydroxide (CH) generated during cement hydration, creating a tri-calcium silicate hydrate (CSH) [26, 27]. This compound will exhibit hardness, strength, stability, and the capacity to fill microcracks and voids, resulting in significant improvements in the strength and durability of concrete [22]. The allowable percentage of cement that can be replaced by SCMs is determined by the type and quantity of active SiO₂ found in the SCMs. Determining the optimal replacement or addition percentage is crucial to facilitate the chemical reaction between SiO2 and CH in concrete mixtures. For instance, replacing 22% of cement with SF containing 90% SiO₂ can completely consume all CH in concrete within 65 days [28, 29]. If the quantity of SCMs employed as a replacement for cement exceeds the amount required to react with CH, they may serve as fillers, occupying voids and small cracks. An additional increase in the amount of SCM material leads to a decrease in the strength of the concrete [30]. According to ACI 318M-19 [31], the maximum allowable percentage of FA or other natural pozzolanic materials that can replace cement in exposed concrete is 25%. The maximum allowed percentage for the combined utilization of FA or another natural pozzolanic material and SF as a replacement for cement is 35%. Furthermore, it is essential to highlight that under no circumstances should the quantity of SF exceed more than 10% of the cement's weight. The European standards EN 197-1 [32] restrict the amount of FA that can replace the cement to 35% by weight. This limitation is imposed because, at greater levels of FA incorporation, the majority of the FA functions more as a filler rather than a binder material.

Adding steel fiber (STF) to concrete can significantly enhance its mechanical characteristics [33]. Although the compressive strength increased slightly in low STF percentage, the splitting strength, flexural strength, ductility, compressive toughness, and flexural toughness will significantly improve [34]. Adding more than one SCMs, such as SF with FA or KA, combined with STF, in concrete mixes can enhance all concrete properties [35].

Previous studies have determined that the ideal proportion of cement replacement with SF falls between 10% and 15% [36, 37], while for FA, it ranges from 10% to 25% [38, 39]. However, in the case of KA, the optimal range is narrower, specifically between 4% and 5% [40, 41]. By using SCMs alongside cement instead of substituting them, raising the proportion of SCMs is feasible because cement hydration produces more CH than when SCMs replace cement directly.

Previous studies have frequently incorporated STF into concrete mixtures, typically within a range of 0% to 2% of the total concrete volume [34, 42]. The addition of STF to concrete mixes can improve various mechanical properties, including compressive strength, splitting strength, flexural strength, compressive toughness, ductility, flexural toughness, impact energy, delay of the first crack under flexural load, and reduction of crack spacing [43]. A positive correlation exists between the percentage of STF and the compressive strength of concrete, particularly within the range of 0% to 2% of the concrete's total volume. The efficiency of STF is determined by the strength of the concrete and the properties of the STF itself, including its diameter, length, tensile strength, shape, and surface roughness [44]. Adding high amounts of STF into normal-strength concrete is an ineffective approach. The

purpose of STF in concrete under tensile stress is to help alleviate part of the tensile stress, since concrete has a limited ability to withstand it. If the concrete or STF experiences tensile failure or if the STF becomes detached from the concrete because of adhesion failure between the two materials, the concrete cube, cylinder, or beam will begin to develop cracks until it ultimately fails [45]. This study investigates the properties of concrete, which range in strength from normal to high strength. The STF content employed in this study was 0.5% of the total volume of concrete. While SF, FA, KA, and STF have been widely studied for their individual and combined applications in construction materials, their collective impact on treated RAC has received less attention. This gap motivated our current research to explore the synergistic effects of SF, FA, KA, and STF in TRA concrete. Our findings aim to make construction more affordable and environmentally friendly, aligning with development goals.

2. EXPERIMENTAL WORKS

2.1 Materials

This study utilized natural granite aggregate (NA) with a nominal size of 14 mm for the normal concrete mix. The granite aggregate possesses a specific gravity of 2.67 and a water absorption rate of 0.41%. The RA were obtained from waste concrete debris in the form of cubes, beams, and arches that had been tested in earlier studies and subsequently exposed to natural environmental conditions, including rainfall and temperature variations, for more than five years. These waste concrete elements, originally exhibiting compressive strengths between 30 and 40 MPa, were crushed to the required aggregate size using a crushing machine in the Universiti Sains Malaysia (USM) laboratory. The RA underwent a washing process using water on a sieve with a diameter of 4.76 mm to remove dust and small particles of aggregate. The RA was subjected to chemical treatment by immersion in a 0.1 M HCl solution for 24 hours. During this process, HCl reacted with the cementitious mortar, particularly CH, which formed soluble calcium chloride (CaCl₂). The resulting solution exhibited a pH of 6.5 and 7.5, indicating a nearly neutral condition that poses no significant risk when discharged into sewage at a laboratory scale. However, dilution with water may be advisable for larger volumes. Following the treatment, the RA was thoroughly rinsed with water through a 4.76 mm sieve to remove detached fine particles and residual acid. The aggregates were then dried by applying airflow across their surface. The nominal size of the treated recycled aggregate (TRA) was 12.5 mm, and the minimum size was 4.76 mm. The specific gravity was 2.428, and the water absorption was 4.4%. Figure 1 illustrates the sieve analysis results for NA and TRA. The study used river sand (RS) as fine aggregate, with particles passing through a sieve with a 4.76 mm opening and retained on a sieve with a 0.076 mm opening, as shown in Figure 2. The RS's specific gravity, water absorption, and fineness modulus are 2.607,0.99, and 3.1, respectively.

The study utilized ordinary Portland cement (OPC) named CEM I, 52.5 N. The SCMs included SF, FA, and KA, with their chemical composition and scanning electron microscope (SEM) analyses tested at the Earth Material Characterization laboratory at the Centre for Global Archaeological Research,

University Sains Malaysia (USM). The chemical composition of the cement and the SCMs is detailed in Table 1. The SEM test was utilized to analyze the shape and morphology of the OPC, SF, FA, and KA particles. Figure 3 displays the SEM image results that were obtained.

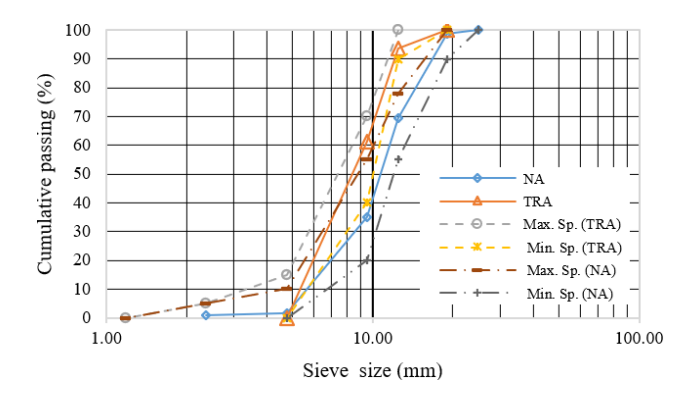


Figure 1. Sieve analysis results of natural and treated recycled aggregate

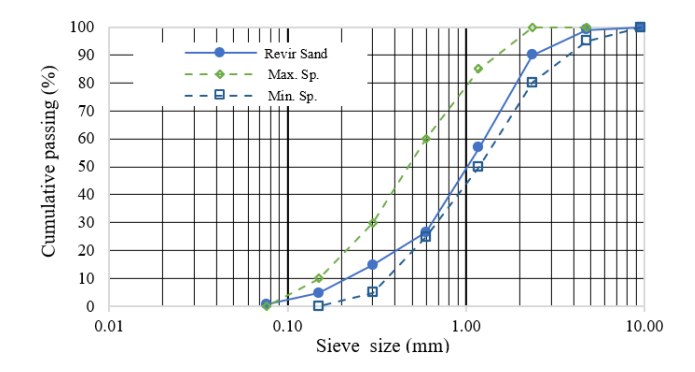


Figure 2. Sieve analysis results of river sand

Table 1. Chemical composition of ordinary Portland cement, silica fume, fly ash, and kaolin

Oxide	OPC	SF	FA	KA
	(%)	(%)	(%)	(%)
SiO ₂	19.52	95.59	54.36	54.32
Al_2O_3	4.97	0.26	25.00	30.24
Fe_2O_3	3.64	0.06	6.15	1.71
CaO	64.32	0.10	5.52	0.01
MgO	2.00	0.33	1.53	1.46
K_2O	0.55	0.62	1.29	5.62
Na ₂ O	0.10	0.36	0.68	0.07
TiO ₃	0.00	0.00	1.21	0.71
P_2O_5	0.04	0.08	0.86	0.02
MnO	0.01	0.00	0.01	0.00

The ImageJ software is employed to analyze SEM pictures to determine the particle size. The cement utilized in this investigation demonstrates an uneven morphology and a coarse texture, with a minimum particle size of $1\mu m$ and a maximum particle size of $100\mu m$. However, over 90% of the particles are smaller than $10~\mu m$. The size of the densified SF varied between $10~and~250~\mu m$, with more than 75% of the particles being less than $100~\mu m$. The densified SF particles exhibited a smooth and spherical shape (Densified silica fume consists of agglomerates formed by processing very fine individual silica fume particles into larger clusters). The FA showed a size distribution ranging from 1 to 12 μm , with over 93% of particles measuring less than $5~\mu m$. The FA had a round and smooth shape. The SEM picture for KA shows an

irregular and rough surface. The KA size ranged from 4 to 30 μ m, with over 68% of particles measuring less than 10 μ m.

Straight and smooth STF with average diameter, length, and aspect ratio of 0.2 mm, 13 mm, and 65 were added to the

concrete mixes. STF was added at a percentage of 0.5% of the concrete volume. According to the manufacturer's catalog, the STF used in this investigation has a tensile strength of 2850 MPa and a density of 7900 kg/m^3 [46].

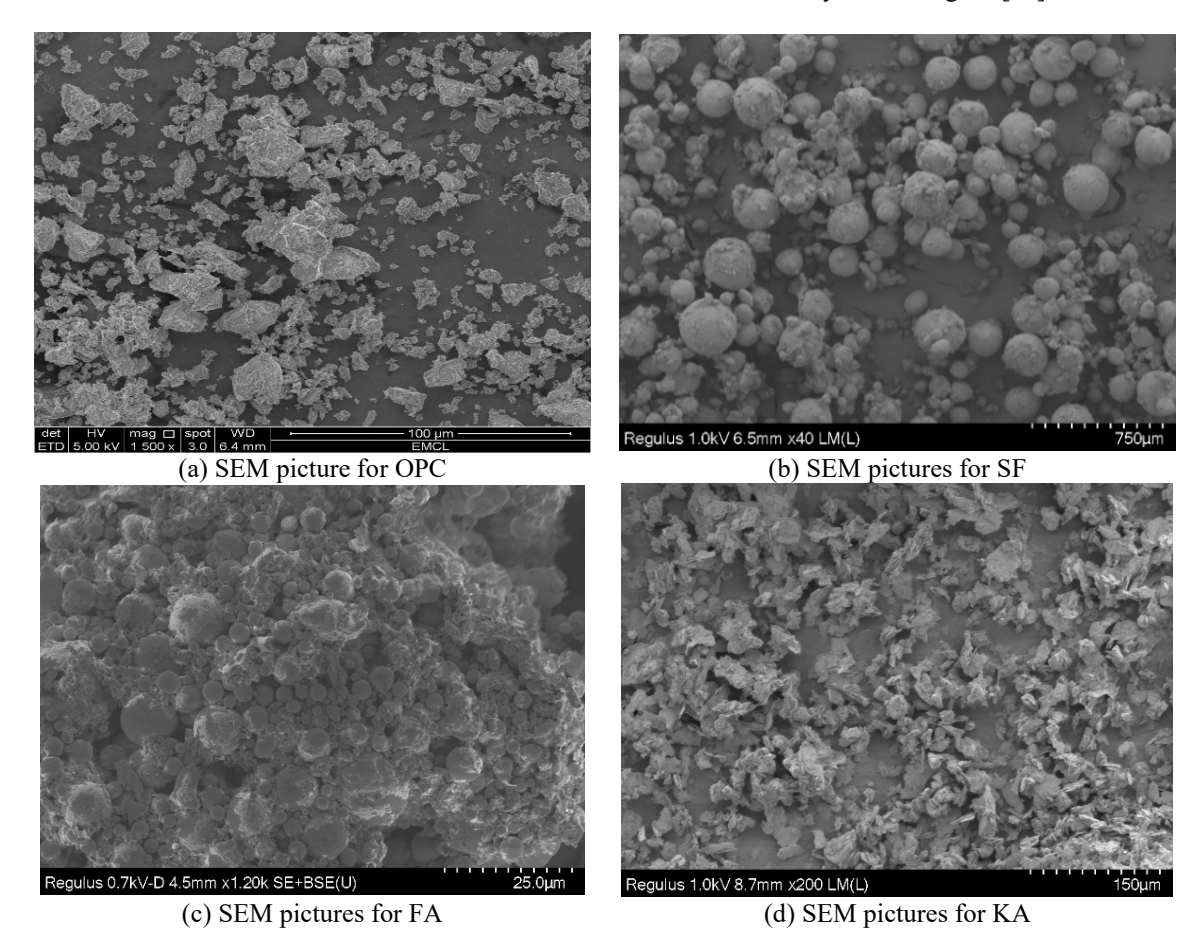


Figure 3. Scanning electron microscope (SEM) pictures for OPC, SF, FA, and KA

2.2 Mixing procedures

This study employed the two-stage mixing approach (TSMA) to mix concrete ingredients. The mixing process consists of five steps. Firstly, the total quantities of sand and aggregate were combined with half the water, and the mixer was operated for one minute. Second, the cement and SCMs were added, and mixing continued for two more minutes. Third, the remaining water and the superplasticizer were incorporated, and mixing proceeded for another three minutes. Fourth, the mixer was halted for one minute. Fifth, mixing was resumed for three minutes. Lastly, the mixture was ready [47].

2.3 Specimens shape, molding fresh concrete, and treating hardened concrete

A cube with a size of 100 mm specimens was utilized to measure the concrete's compressive strength, water absorption, porosity, and density [48]. Cylindrical specimens of 100 mm in diameter and 200 mm in height were employed to determine the splitting strength and modulus of elasticity [49]. The third-point loading of flexural strength tests was conducted using specimen dimensions of $100 \times 100 \times 500$ mm. The specimens with similar dimensions were also utilized for impact load tests [50]. The water permeability of concrete was evaluated using cylindrical specimens of 50 mm in diameter and 40 mm in height. These specimens were prepared from

cube or beam samples using a core machine. A cylindrical specimen of 100 mm in diameter and 50 mm in height was used to perform the rapid chloride permeability (RCP) test [51]. After mixing the concrete gradients, a slump test was performed according to the standards specified in ASTM C143 [52]. Afterwards, the freshly mixed concrete was cast into the specified molds according to the specifications outlined in the ASTM C192 standard [53]. The freshly molded concrete was compacted using a vibration table apparatus. The concrete sample molds were kept at room temperature, ranging from 23 to 31 degrees Celsius, and covered with a moist cloth for 24 hours. Subsequently, the concrete molds were de-molded, and the concrete samples were submerged in a water treatment tank maintained at a temperature range of 23-27 degrees Celsius until the specified testing days (7, 28, 56, and 96 days) [53].

2.4 Mix proportion design

This study used the ACI211.1 standard [54] for concrete mix design, specifically focusing on the absolute volume technique. The SA, FA, and KA were used as additional quantities rather than replacements for the cement. As a result, the amounts of concrete ingredients were adjusted to equal a volume of 1 cubic meter. Table 2 provides a detailed description of the composition of eight different concrete mixes.

Table 2. Mixing proportions for conventional and treated

Mi Cada	Material (Kg/m³)								
Mix Code	\mathbf{CM}	SF	FA	KA	STF	WT	RA	RS	SP
N1	444	-	-	-	-	211	900	772	-
R1	444	-	-	-	-	206	940	637	2.2
R2-STF0.5	444	-	-	-	39	206	940	637	2.2
R3-STF0.5-SF10	444	44.4	-	-	39	226	940	637	3.3
R4-STF0.5-FA15	444	-	66.7	-	39	236	940	637	3.3
R5-STF0.5-KA5	444	-	-	22.2	39	216	940	637	3.3
R6-STF0.5-SF10-FA15	444	44.4	66.7	-	39	256	940	637	3.3
R7-STF0.5-SF10-KA5	444	44.4	-	22.2	39	236	940	637	3.3

Notes: N: normal concrete with granite aggregate, R: concrete with TRA, the numerical values following "N" and "R" correspond to the sequential job mix number, the numbers following "STF," "SF," "FA," and "KA" indicate the respective percentages of these materials added to the concrete mixture.

WT: Total water, CEM: Cement.

2.5 Tests of fresh and hardened properties of concrete

The slump test was conducted following the guidelines of the ASTM C143 standard [52]. The saturated and surface dry density, absorption, and porosity of the hardened concrete were determined through tests and calculations that followed the specifications mentioned in the ASTM C 642 standard [48]. The water permeability of concrete was assessed and computed according to the methodology described in the research by Hedegaard and Hansen [55]. The rapid chloride permeability test was performed and computed according to the ASTM C 1202 specifications [56]. The hardened concrete's compressive strength was tested following BS-EN-12390-3-2019 [57] at several ages, particularly 7, 28, 56, and 96 days, utilizing 100 mm cubes. The hardened concrete's splitting tensile strength was measured at 28 days using the methods outlined in ASTM C496 [58]. The cylindrical compressive strength, static modulus of elasticity, Poisson's ratio, and compressive toughness for concrete were measured using the ASTM C 469 standards [49] at age 28 days. To quantify the vertical and transverse strains of the concrete cylinder samples, it is imperative to attach two strain gauges to each sample's vertical and transverse surfaces. The strain gauges used are KYOWA type, with a length of 60 mm, which are made in Japan [49]. Flexural strength was assessed following ASTM C78 and ASTM C 1609/C1609M-19 [59], utilizing a third-point loading method in which two loads were applied to the upper surface of the concrete specimen. The distance from the support to the load was 100 mm, which is one-third of the distance between the supports. This test yielded results for flexural strength and flexural toughness [50, 59]. The flexural impact energy of the hardened concrete beams was evaluated after 28 days using a process previously described in the research conducted by Noaman et al. [60] and Hao et al. [61]. where the sample size was $100 \times 100 \times 500$ mm, the drop weight was 4.54 kg, the falling drop height was 200 mm, and the sample span was 400 mm.

3. RESULTS AND DISCUSSION

3.1 Slump

The results of the slump test are illustrated in Figure 4, showing that all eight mixes in this study exhibited true (normal) slump shapes. Moreover, the R1 mix displayed a significantly higher slump value than N1. Specifically, N1

exhibited a slump value of 70 mm, while R1 recorded 120 mm, representing a 71.4% increase compared to N1.

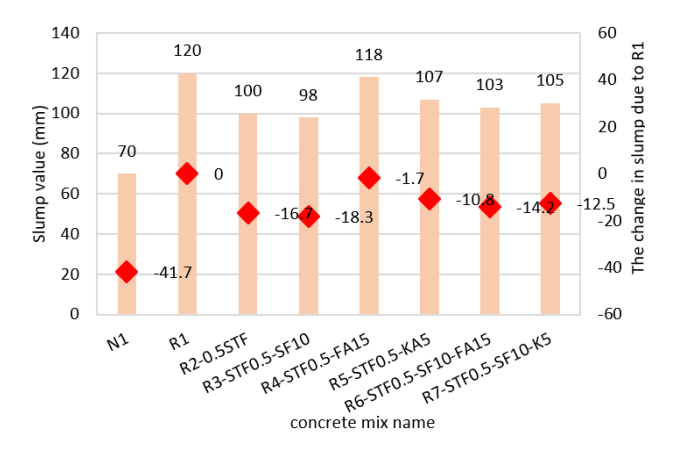


Figure 4. Slump test results

Studies indicate that replacing NA with RA without a workability admixture generally reduces slump due to RA's high-water absorption [62]. However, the improved slump value of R1 compared to N1 can be attributed to the synergistic effects of using well-graded saturated and surface dry TRA [63], the addition of 0.5% superplasticizer [64], and the TSMA in concrete mixing [65].

Using well-graded RA enhanced packing density, reduced voids, and minimized water demand, while its saturated and surface dry condition prevented additional water absorption during mixing, ensuring consistent workability [63]. The superplasticizer dispersed cement particles, reduced friction, and compensated for the rough texture of RA, significantly improving fluidity [64]. TSMA further optimized the mix by ensuring a uniform coating of aggregates and effective integration of the superplasticizer [66]. Together, these factors mitigated the typical drawbacks of RA, such as higher absorption and roughness, resulting in a concrete mix with superior workability and a higher slump value than N1.

Furthermore, to observe the effect of STF, a comparison between R2-0.5STF and R1 shows that adding 0.5% STF to the mix reduces the slump value by approximately 19.2%, as shown in Figure 4. The slump reduction in the R2-0.5STF mix can be attributed to the increased inter-particle friction and disruption of paste flow caused by the addition of STF [67].

Although adding 0.5% superplasticizer can enhance workability, it is insufficient to completely counteract the effects of STF, resulting in a lower slump value. Therefore, it is crucial to carefully adjust the mix proportions and admixture dosage when incorporating STF to achieve the desired workability.

Kőksal et al. [68] investigated the relationship between STF dosage and concrete slump, finding that incorporating 0.5% STF by volume reduced slump by 16.7%, which closely aligns with the findings of this study.

Including SCMs such as SF, FA, or KA, or integrating STF alone or in combination, significantly reduces the slump value of concrete mixes [69]. To minimize slump reduction and maintain a target slump above 70 mm, the superplasticizer dosage had to be increased to 3.3 kg/m³ in concrete mixes containing SCMs or STF. This adjustment ensured that the mixes met the required workability criteria while preserving consistency and performance.

The slump values for concrete incorporating treated recycled aggregate ranged from 98 mm to 120 mm, with slump

reductions between 1.7% and 18.3%, as shown in Figure 4.

3.2 Water absorption, water permeability, and porosity

The water absorption, porosity, and water permeability of the eight mixes were tested on day 28, and the results are shown in Table 3. The absorption percentage and porosity of R1 were 4.50% and 9.90%, respectively, representing increases of 11.11% and 7.61% compared to N1. However, the increase is insignificant compared to N1.

Table 3. Water absorption, porosity, and water permeability results

	ABS	ΔABS	n	Δn	K	ΔK
Mixture Code	(%)	(%)	(%)	(%)	$(\times 10^{-11} \text{ m/s})$	%
N1	4.05	-	9.20	-	2.07	-
R1 (Ref.)	4.50	0.00	9.90	0.00	2.93	0.00
R12-STF0.5	4.32	-4.00	9.60	-3.00	2.79	-4.50
R13-STF0.5-SF10	3.02	-32.90	6.65	-32.80	0.74	-74.70
R14-STF0.5-FA15	3.76	-16.40	8.20	-17.20	1.08	-63.10
R5-STF0.5-KA5	3.98	-11.60	8.75	-11.60	1.53	-47.70
R6-STF0.5-SF10-FA15	2.78	-38.20	6.15	-37.90	0.54	-81.50
R7-STF0.5-SF10-KA5	2.86	-36.40	6.24	-37.00	0.63	-78.50

Note: ABS is the concrete water absorption; n is the concrete porosity; K is the concrete water permeability; Δ is the percentage of change.

The primary factor contributing to the slight difference in water absorption between N1 and R1 is the treatment procedure used for RA, which effectively removes a substantial amount of weak mortar. This finding aligns with a study by Güneyisi et al. [70], which demonstrated that treating RA with 0.1 M HCL can decrease the water absorption and porosity in RAC by 11% to 20%.

The water permeability of R1 increased by 41.55% relative to N1. This heightened water permeability is primarily due to the old cement mortar, which remained firmly adhered to the aggregate and exhibited a significant permeability. Additionally, grinding the concrete debris led to the degradation of the interfacial transition zone (ITZ) between the aggregate and the pre-existing mortar of some aggregate particles, resulting in a weaker ITZ compared to that between the aggregate and the new mortar, which contributed to an increase in the concrete porosity, water absorption, and water permeability [10].

A comparison between R2-STF0.5 and R1 revealed that adding 0.5% STF to the concrete reduced the porosity, water absorption, and water permeability by 4.00%, 3.00%, and 4.50%, respectively. This reduction was attributed to decreased shrinkage and creep, which lowered the quantity and size of microcracks [71]. However, the decrease was relatively small due to the lack of chemical interaction between the STF and OPC in the concrete mixture [72].

Incorporating STF in TRAC, alongside SCMs such as SF, FA, and KA, significantly reduced the porosity, water absorption, and water permeability, thereby enhancing concrete durability. The test results for water absorption, porosity, and water permeability, along with their percentage reductions relative to R1, are summarized in Table 3.

SCMs contain varying amounts of SiO₂, which reacts with CH during cement hydration. This reaction forms CSH, a dense, water-insoluble compound that effectively fills voids and microcracks within the concrete matrix, enhancing its stability and durability [73]. The SCMs used in this study had significant fineness, allowing them to seal microcracks in the

old ITZ efficiently [74]. Consequently, the concrete produced had a high density and very few voids, leading to reductions in concrete porosity, water absorption, and water permeability [75].

Adding two SCMs alongside STF in R6-STF0.5-SF10-FA15 and R7-STF0.5-SF10-KA5 significantly decreased concrete porosity, water absorption, and water permeability compared to R1. The water absorption values for these two mixes declined by 38.20% and 36.40%, respectively. Similarly, porosity decreased by 37.90% and 37.00%, while water permeability decreased by 81.50% and 78.50%, respectively.

The primary cause of these reductions was the high SCMs content, accounting for 25% and 15% of the cement's weight, which consumed most of the CH generated during cement hydration. This process led to the formation of CSH, effectively filling voids and small cracks in the concrete [76].

Qureshi et al. [77] found that replacing 10% of cement with SF and including 1% STF (by total concrete volume) resulted in a 27.6% reduction in water absorption compared to RAC. Lin et al. [78] examined the impact of replacing 10% of cement with SF and adding 0.5% STF on concrete water absorption, noting a 44.4% reduction compared to conventional concrete. Akhtar et al. [79] reported that replacing 15% of cement with FA and adding 0.5% STF led to a 29.29% decrease in water absorption compared to conventional concrete.

The present study aligns with prior research; however, earlier studies primarily used natural aggregate as coarse aggregate, further supporting the efficacy of the treatment technique employed in this study.

3.3 Rapid chloride permeability test

Figure 5 and Figure 6 illustrate the RCP test results and the RCP values normalized against R1 at 28 and 96 days. The RCP values for N1 were 3449 Coulombs at 28 days and 2653 Coulombs at 96 days, both categorized as moderate [51]. The decline in the RCP value between the two ages may be ascribed to the continuous process of cement hydration and the formation of CSH. This compound effectively plugs voids and microcracks, reducing the porosity, water absorption, and permeability, and decreasing the RCP value [80].

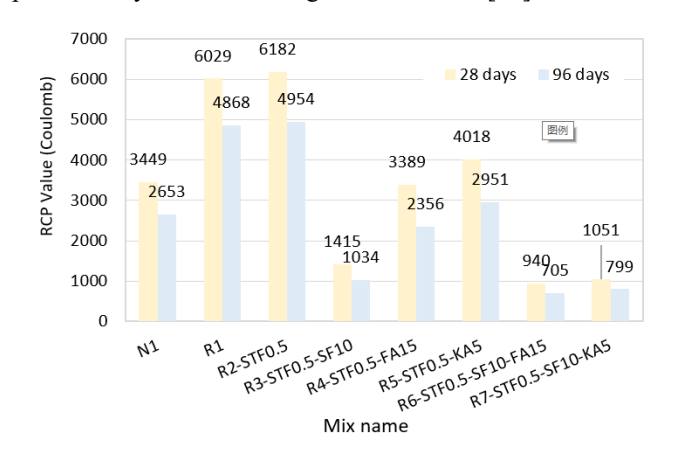


Figure 5. Results of RCP test

The R1 mix showed RCP values of 6029 coulombs at 28 days and 4868 coulombs at 96 days. These values are considered high according to the ASTM C1202 standard [56]. The RCP value for R1 increased by 74.80% and 83.49% at 28 and 96 days, respectively, compared to N1. The increase in the

RCP value for R1 may be attributed to its higher absorption, porosity, and permeability than N1, in addition to the presence of microcracks in the old mortar, which attached to the recycled aggregate, resulting in an elevated penetration of chloride ions [81].

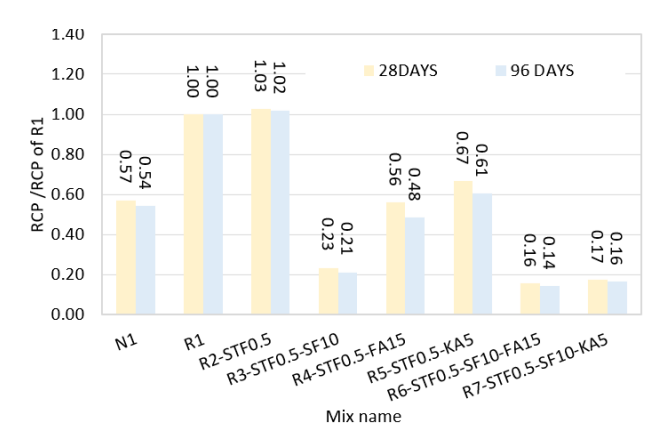


Figure 6. RCP test results normalized by the RCP value of R1

Adding 0.5% STF to the R2-STF0.5 mix increased the electrical conductivity of the concrete, leading to a higher RCP value [82]. In the R3-STF0.5-SF10 mix, incorporating 10% SF (by cement weight) and 0.5% STF (by total volume) significantly reduced RCP values by 76.53% at 28 days and 78.76% at 96 days, compared to TRAC samples. Similarly, adding 15% FA or 5% KA (by cement weight) with 0.5% STF in R4-STF0.5-FA15 and R5-STF0.5-KA5 further reduced RCP values. At 28 days, reductions were 43.8% (FA) and 33.4% (KA), while at 96 days, the decreases reached 51.6% and 39.4%, respectively, relative to R1.

The combination of two SCMs as 10% SF with either 15% FA or 5% KA, along with 0.5% STF, significantly decreased RCP values in the concrete mixtures R6-STF0.5-SF10-FA15 and R6-STF0.5-SF10-KA5. At 28 days, the RCP values decreased by 84.4% and 82.6%, respectively, while at 96 days, the reductions further increased to 85.5% and 83.6%.

The incorporation of SF in concrete significantly reduces RCP compared to FA or KA, particularly at early ages (28 days). This reduction is attributed to the higher SiO₂ content and greater chemical reactivity of SF compared to FA and KA. Adding 0.5% STF with two SCMs, either 10% SF + 15% FA (totaling 25%) or 10% SF + 5% KA (totaling 15%), further enhances this effect. The increased SiO₂ concentration reacts with CH to form CSH, a robust and durable compound that fills voids and microcracks, leading to substantial reductions in water absorption, porosity, and water permeability, which are key factors contributing to the observed RCP decline [83].

Kumar and Rai [39] reported that replacing 10% of cement with SF and 15% with FA reduced RCP to 1100 Coulombs, which aligns closely with the findings of this study. Similarly, Kumar and Anandhi [84] investigated the combined effects of various SCMs, including SF, FA, and KA, with total replacement levels of 15% and 22.5% of cement weight. The findings revealed substantial declines in RCP values, 43.70% and 75.73%, respectively, for normal aggregate concrete, demonstrating the high effectiveness of the recycled aggregate treatment method adopted in this study, as well as the application of the TSMA technique.

The current research outcomes are consistent with previous studies, with minor variations. These discrepancies may be attributed to the higher SCM quantities used in this study, whereas earlier research focused solely on partial cement replacement.

3.4 Relationship between absorption, porosity, and permeability with rapid chloride permeability

Eq. (1) to Eq. (3) illustrate the linear and proportional relationships between the water absorption (ABS, %), porosity (n, %), and water permeability (K, \times 10⁻¹¹ m/s) with RCP (Coulombs), as depicted in Figure 7, Figure 8, and Figure 9.

$$RCP = 2964.1 \times ABS - 7536$$
 (1)

$$RCP = 1296.9 \times n - 7177.9$$
 (2)

$$RCP = 2066.6 \times K + 129.07$$
 (3)

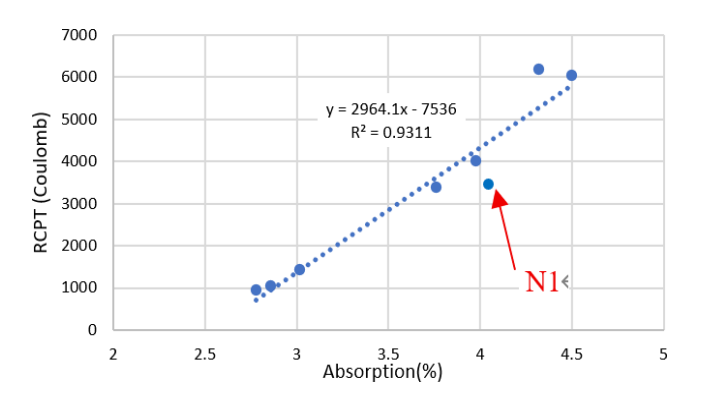


Figure 7. The relationship between the water absorption percentage and the rapid chloride permeability

Figure 7 illustrates the relationship between water absorption and RCP results. The positive linear trend suggests that as absorption increases, RCP values also rise, indicating higher chloride ion penetration in concrete with greater water absorption. The regression Eq. (1) suggests that for each 1% increase in water absorption, the RCP value increases by approximately 2964 Coulombs. The coefficient determination ($R^2 = 0.9311$) demonstrates a strong correlation between water absorption and RCP, implying that 93.11% of the variation in RCP results can be explained by changes in water absorption. The outlier observed in the three figures corresponds to mix N1, which incorporates natural aggregate exhibiting distinct characteristics compared to TRA, thereby accounting for the observed deviation. This trend highlights that concrete with lower water absorption tends to show better durability and lower water permeability, emphasizing the importance of optimizing mix design to minimize water absorption and improve long-term performance against chloride-induced deterioration.

Figure 8 illustrates the relationship between concrete porosity and RCP results. The positive linear correlation suggests that as the porosity increases, the RCP values also rise, indicating greater chloride ion penetration in more porous concrete. The regression Eq. (2) indicates that for each 1% increase in porosity, the RCP value increases by approximately 1296.9 Coulombs. The coefficient of determination ($R^2 = 0.9104$) demonstrates a strong correlation, meaning that 91.04% of the variation in RCP values can be explained by changes in porosity. This trend highlights that concrete with higher porosity tends to have lower resistance to

chloride penetration, emphasizing the need for optimized mix designs that reduce porosity to enhance durability and long-term performance against chloride-induced deterioration.

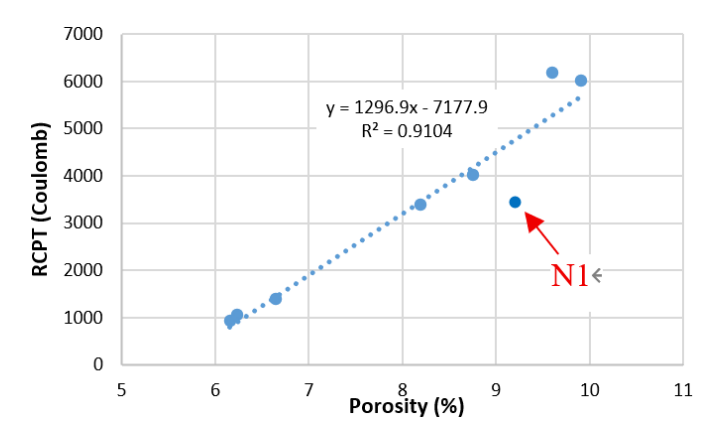


Figure 8. The relationship between the porosity percentage and rapid chloride permeability

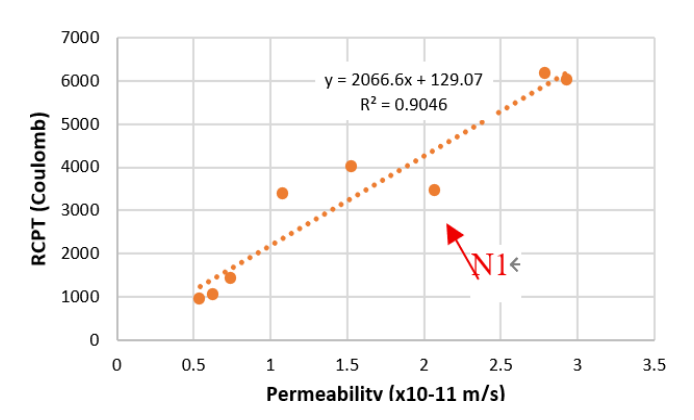


Figure 9. The relationship between the water permeability and rapid chloride permeability

Figure 9 illustrates the relationship between water permeability and RCP results. The positive linear correlation suggests that as water permeability increases, RCP values also rise, indicating greater chloride-ion penetration in concrete with higher permeability. The regression Eq. (3) indicates that for each increase of 1×10^{-11} m/s in the water permeability, the RCP value increases by approximately 2066.6 Coulombs. The coefficient of determination ($R^2 = 0.9046$) demonstrates a strong correlation, meaning that 90.46% of the variation in RCP values can be explained by changes in water permeability. This trend highlights that concrete with higher water permeability tends to be more susceptible to chloride ingress, emphasizing the need for improved mix designs and material modifications to reduce permeability and enhance long-term durability.

This study demonstrates an innovative approach to enhancing concrete performance by combining recycled concrete aggregate, fly ash, silica fume, kaolin, and STF. Beyond its technical contribution, the strategy holds notable interdisciplinary significance, offering a practical pathway to alleviate construction waste while supporting sustainable waste management practices. Moreover, by improving durability, the findings highlight the potential to extend infrastructure service life, minimize maintenance demands, and ultimately lower the long-term carbon footprint, contributing to more sustainable urban development.

3.5 Compressive strength

The compressive strength was measured at four different time intervals: 7, 28, 56, and 98 days, as illustrated in Table 4. R1 exhibited reductions in compressive strength of 4.52%, 4.44%, 3.99%, and 3.77% compared to N1 at the same specified ages. The reduction in compressive strength for R1 was negligible, remaining below 5%, which can be attributed to the utilization of well-graded aggregate and the removal of a substantial quantity of old mortar during the crushing process to achieve the intended aggregate size. Moreover, the treatment process involved immersing the aggregate in hydrochloric acid, while the concrete mixing process incorporated the use of the TSMA [85].

Adding 0.5% STF to the R2-STF0.5 concrete mix increased the compressive strength by 3.66%, 5.42%, 5.38%, and 5.03% at 7, 28, 56, and 98 days, respectively. The observed increase in compressive strength is strongly supported by previous investigations, which showed that adding 0.5% STF resulted in a 6.82% and 8.51% enhancement in the compressive strength after 28 and 90 days, respectively [86]. The incorporation of STF enhances compressive strength due to its ability to resist and mitigate microcracks that form under tensile stress caused by compressive loads [87].

Using a combination of 10% SF, 15% FA, or 5% KA along with 0.5% STF in concrete mixes R3-STF0.5-SF10, R4-STF0.5-FA15, and R5-STF0.5-KA5 significantly improved compressive strength at each tested age, as illustrated in Table 4. A notable enhancement in compressive strength was observed when 0.5% STF and two SCMs were added to the concrete mixes R6-STF0.5-SF10-FA15 and R7-STF0.5-SF10-K5. At 7 days, the compressive strength increased by 28.05% and 23.88%, respectively. Similarly, at 28 days, the compressive strength improved by 28.92% and 24.58%, respectively. By 56 days, the increases were 27.06% and 23.94%, respectively. Finally, at 98 days, the strength rose by 25.83% and 22.6%, respectively.

The significant improvement in the compressive strength correlates closely with the high SCM content, especially 25% (10% SF with 15% FA) and 15% (10% SF with 5% KA).

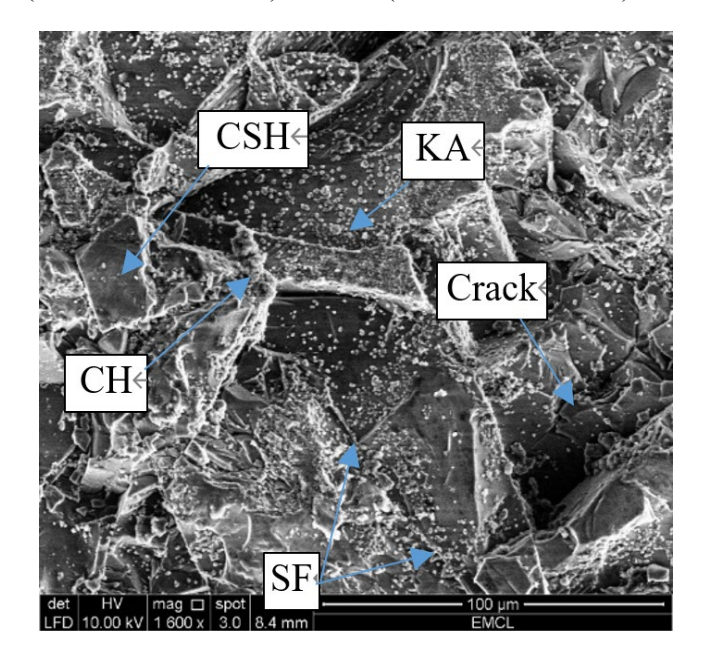


Figure 10. SEM image for concrete mix containing SF and KA

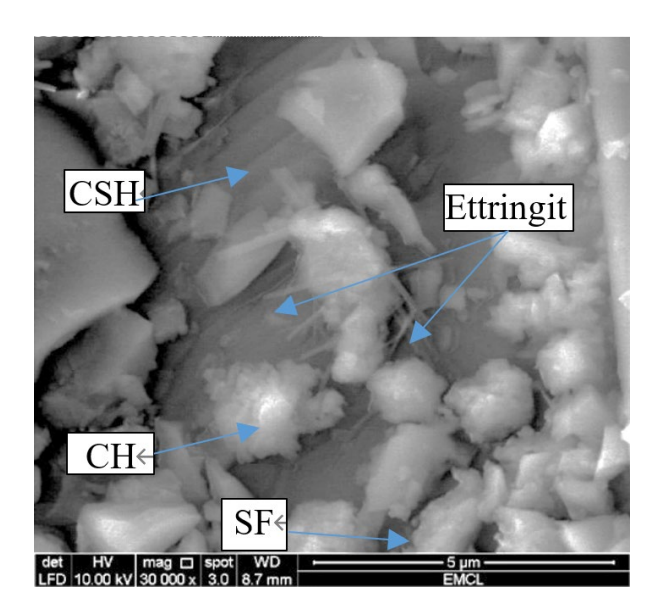


Figure 11. SEM image for concrete mix containing SF

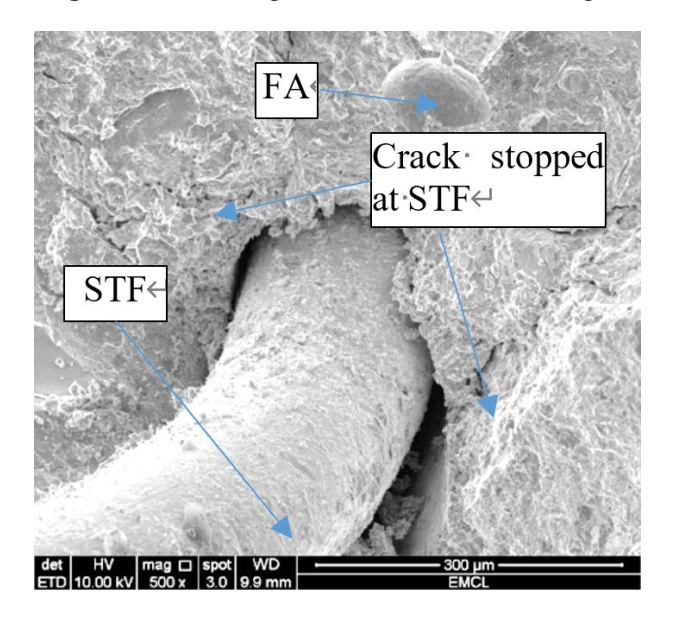


Figure 12. SEM image for concrete mix containing STF

Qureshi et al. [86] investigated the effect of incorporating two SCMs, namely 10% SF and 15% FA, into concrete. Their findings showed a 21.96% increase in the compressive strength after 28 days. Similarly, Kumar and Rai [39] reported

that the combined addition of 10% SF and 15% FA improved the compressive strength by 22.17% compared to the reference mix containing natural aggregate, with the reported value being the average of mixes with 10% and 20% FA. These results closely align with the outcomes of the present study; however, whereas previous studies employed natural aggregate, the current research used TRA, highlighting TRA's effectiveness in enhancing concrete performance.

SCMs consume most of the CH through chemical reactions during cement hydration, leading to the formation of CSH. This dense, strong, and durable compound fills voids and microcracks, thereby improving compressive strength, as explained in microstructure SEM images in Figures 10 and 11. Furthermore, adding STF to concrete enhances its tensile strength by delaying and stopping the formation of microcracks induced by compressive stresses, which is explained by the microstructure SEM image in Figure 12 [76].

A regression analysis established the relationship between compressive strength, curing age, and the proportion of amorphous silica within the total binder content, as expressed in Eq. (4). The model achieved a coefficient of determination (R²) of 0.97, signifying that nearly 97% of the variation in compressive strength is accounted for by the selected parameters, namely the logarithm of curing age and the percentage of active silica. This high degree of correlation indicates strong agreement between experimental and predicted values, underscoring the reliability of the proposed equation in capturing the combined effects of material composition and curing duration. Consequently, the regression model proves to be a robust approach for predicting the strength development of modified concrete mixtures.

The general expression for calculating the amorphous SiO₂ content is given in Eq. (5), with Eq. (6) providing an illustrative calculation for a mix containing 10% SF.

$$\sigma_c(\text{MPa}) = 29.4 + 5.95 \times Ln(t) + 0.86 \times S1$$
 (4)

where, t is the concrete age (7, 28, 56, and 96 days); S1 is the percentage of the amorphous silicon oxide compared to the cementitious weight (%).

$$S1 = 100 \times \frac{S2 \times CM_W \times S3 + CM_W \times S4 \times S5}{CM_W + SCM_W}$$
 (5)

Table 4. Compressive strength (σ_c) results and the percentage of change $(\Delta \sigma_{c})$ related to R1

-	7 Days		7 Days 28 Days			56 Da	ys	98 Days	
Mix Code	σ _c (MPa)	Δσ _c (%)	σ _c (MPa)	Δσ _c (%)	σ _c (MPa)	Δ σ _c (%)	σ _c (MPa)	Δσ _c (%)	
N1	$42.40{\pm}1.34$	4.73	51.34±1.41	4.64	54.20 ± 1.74	4.16	56.26 ± 1.54	3.92	
R1	40.48 ± 1.52	0.00	49.06 ± 1.83	0.00	52.04 ± 2.65	0.00	54.14 ± 2.44	0.00	
R2-0.5STF	41.96 ± 1.78	3.66	51.72±2.25	5.42	54.84 ± 2.47	5.38	56.86 ± 2.31	5.03	
R3-STF0.5-SF10	48.84 ± 2.05	20.64	58.37 ± 2.76	18.97	61.65±3.06	18.47	63.55 ± 2.69	17.39	
R4-STF0.5-FA15	45.65 ± 1.89	12.76	56.32 ± 1.66	14.79	60.32 ± 2.37	15.91	63.24 ± 2.11	16.82	
R5-STF0.5-K5	43.98 ± 1.36	8.64	53.87 ± 1.87	9.80	57.22±2.34	9.95	59.67 ± 2.29	10.22	
R6-STF0.5-SF10-FA15	51.84 ± 1.28	28.05	63.25 ± 1.68	28.92	66.12±2.24	27.06	68.12 ± 2.69	25.83	
R7-STF0.5-SF10-KA5	50.15 ± 1.45	23.88	61.12 ± 1.69	24.58	64.50 ± 2.11	23.94	66.37 ± 2.38	22.60	

$$\frac{S1(SF10\%) = 100 \times}{\frac{10\% \times 444kg \times 95.59\% + 444kg \times 19.52\% \times 5\%}{444 + 44.4}}_{= 9.57\%}$$
(6)

where, S2 is the SCMs' percentage (%); CM_W is the OPC weight (kg); S3 is the percentage of amorphous silica oxide in the SCMs (%); S4 is the total percentage of silica oxide in OPC (%); S5 is the percentage of amorphous silica oxide in the OPC (%); SCM_W is the weight of SCMs.

3.6 Splitting strength

The splitting tensile strength was measured after 28 days of standard curing, and the corresponding results are presented in Figure 13. The splitting strength of R1 was almost identical to that of N1, differing by only 1.86%. Ali et al. [88] observed a 9% decrease in the splitting strength of RAC compared to natural aggregate concrete. The differences observed in the current study can be attributed to the use of well-graded TRA, the incorporation of TSMA during mixing, and the comparable compressive strength between TRAC and NC [85].

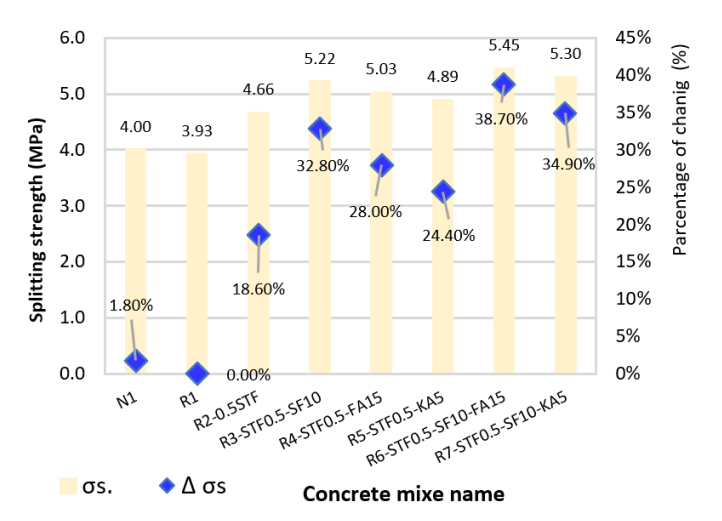


Figure 13. The splitting strength results and the change percentage related to R1

Adding 0.5% STF to the R2-STF0.5 concrete mix resulted in a significant enhancement in splitting strength, increasing by 18.60% compared to R1. Ren et al. [89] found that using 0.5% STF led to an 18.46% increase in the splitting strength, which aligns with the findings of this study. STF improves concrete's resistance to internal tensile stress, enhancing its ability to withstand internal cracks and inhibiting microcrack propagation [87].

Using 10% SF, 15% FA, or 5% KA individually, along with 0.5% STF, resulted in a significant increase in the splitting strength by 32.80%, 28.00%, and 24.40%, respectively. The observed enhancement in the splitting strength is attributed to the inclusion of STF, which resists splitting and tension forces, thereby mitigating crack formation. Additionally, SCMs improve the compressive strength of the concrete, subsequently enhance splitting strength, as discussed earlier.

Qureshi et al. [77] examined the impact of replacing 10% of SF or 20% of FA (by cement weight) while incorporating 1% STF (by total concrete volume). The researchers found that the splitting strength increased by 41.0% and 31.5%, respectively, compared to the conventional concrete mix. The results of the current study closely match previous findings. However,

adding 1% STF resulted in greater enhancement than the present study, which used 0.5% STF.

Adding a combination of 10% SF, 15% FA, and 0.5% STF in the R6-STF0.5-SF10-FA15 mix significantly improved the splitting strength by 38.70% compared to R1. Incorporating 10% SF, 5% KA, and 0.5% STF in the R7-STF0.5-SF10-KA5 mix significantly enhanced the splitting strength, substantially increasing it by 34.9%. Khan and Ali [90] found that adding 10% SF and 15% FA (by cement weight), along with 2% coconut fiber (by total concrete volume), resulted in a 19% enhancement in splitting strength compared to the standard sample. This study aligns with those findings, with the primary difference being the replacement of coconut fiber with STF.

STF exhibits exceptional resistance to tensile stress and effectively prevents microcrack formation. The increase in splitting strength is attributed to the same mechanisms that contribute to compressive strength enhancement. These factors include chemical reactions of SiO₂ in SF, FA, and KA with CH, leading to the formation of CSH. This reaction improves concrete's ability to resist splitting by filling voids and small cracks. Additionally, the use of STF greatly enhances the splitting strength due to its high tensile strength and ability to mitigate microcrack formation [76].

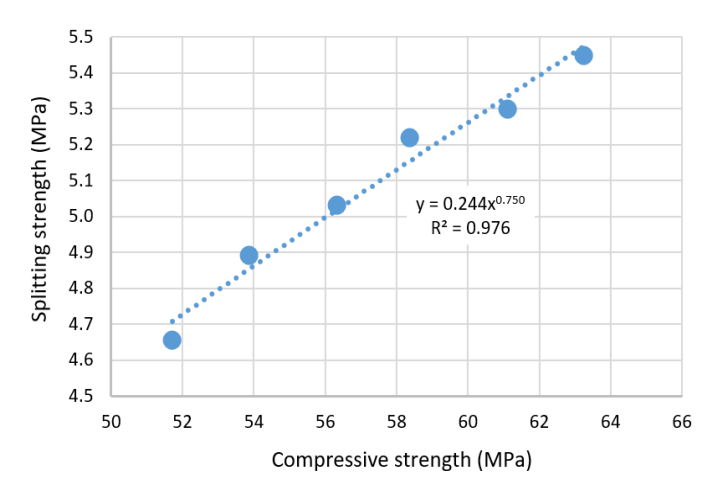


Figure 14. The relationship between compressive strength and splitting tensile strength

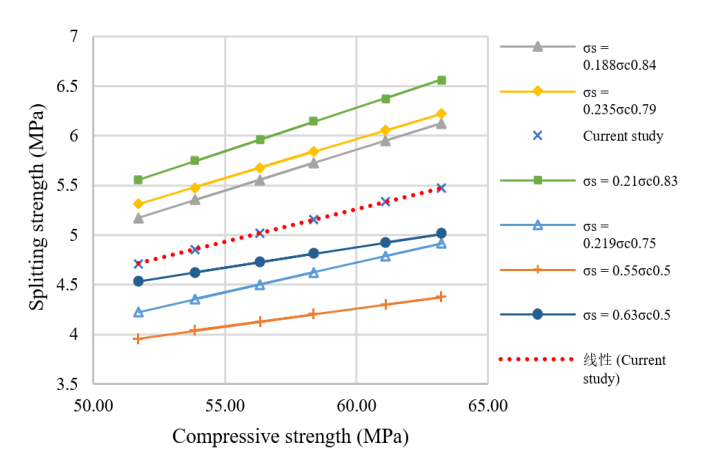


Figure 15. Compressive and splitting strength relationship current vs. prior studies [68, 91-95]

The relationship between the compressive strength (σ_c) and splitting tensile strength (σ_{sp}) in concrete mixes containing SCMs and STF is illustrated in Figure 14, showing a direct, positive correlation. Eq. (7) provides a mathematical

representation of the observed results. Previous studies have extensively examined the correlation between compressive and splitting strengths, demonstrating a positive relationship that can be quantitatively represented by the equation: $\sigma_{sp} = a \times \sigma_c^b$ [91]. The values of variables a and b fluctuate depending on compressive strength, concrete composition, and the inclusion of supplementary components. Figure 15 illustrates the correlation between compressive strength and splitting strength, using data from previous studies alongside the current study's results. The splitting strength curve in this research closely follows the midpoint between the curves of earlier studies.

$$\sigma_{sp} = 0.244 \times \sigma_c^{0.75} \tag{7}$$

3.7 Modulus of elasticity, Poisson's ratio, and compressive toughness

The modulus of elasticity was assessed using three specimens from each concrete mixture. The results of the modulus of elasticity test and the relevant parameters are displayed in Table 5. Furthermore, Figure 16 presents the stress-strain curves for the eight concrete mixtures.

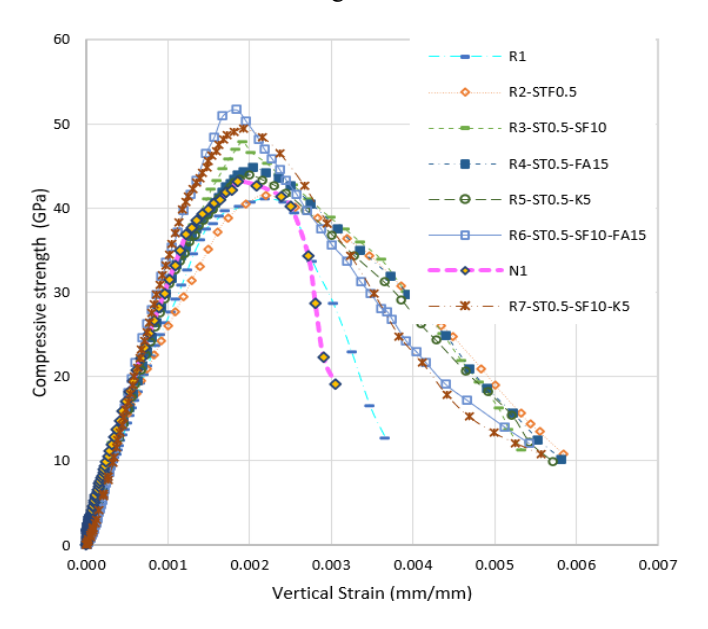


Figure 15. The correlation between vertical strain and cylindrical compressive strength

The modulus of elasticity of the R1 concrete mix exhibited a 5.04% decrease relative to N1. Adding 0.5% STF to the R2-STF0.5 mix enhanced the modulus of elasticity by 4.53% compared to R1. Additionally, using 10% SF, 15% FA, or 5% KA, each combined with 0.5% STF, yielded improvements of 12.38%, 8.79%, and 8.13%, respectively, relative to R1. The inclusion of two SCMs, together with 0.5% STF, in the R6-STF0.5-SF10-FA15 and R7-STF0.5-SF10-KA15 concrete mixes led to respective increases of 13.46% and 12.18% in the modulus of elasticity.

The relationship between the square root of the cylindrical compressive strength $(\sqrt{\sigma_{cy}})$ and the modulus of elasticity (E_c) can be described as a linear correlation, as shown by Eq. (8) and Figure 17.

$$E_c = 4824.7 \times \sqrt{\sigma}_{cy} \tag{8}$$

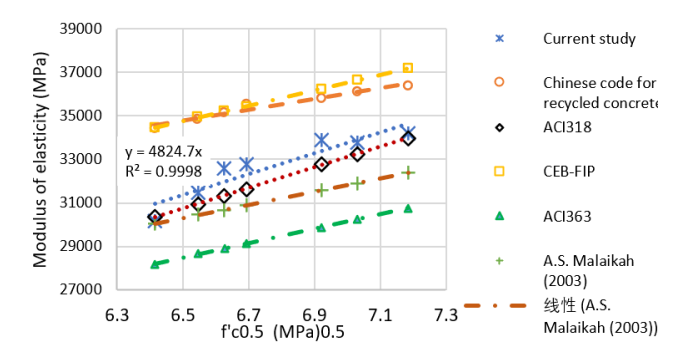


Figure 16. Square root of cylindrical strength versus modulus of elasticity (multiple studies) [96-100]

The ACI 318 code [31] establishes a direct relationship between the cylindrical compressive strength and the modulus of elasticity for normal-weight concrete, as illustrated in Eq. (9). In this study, Eq. (8) presents the derived formula for the modulus of elasticity, specifically for TRAC incorporating SCMs and STF, demonstrating alignment with the ACI 318 code provisions outlined in Eq. (9) [31].

Figure 17 presents the $\sqrt{\sigma_{cy}}$ - E_c curve obtained in this study alongside curves from previous research. The current study's curve lies within the range established by earlier studies [96-100].

$$E_{c} = 4700 \times \sqrt{\sigma}_{cy} \tag{9}$$

Table 5 and Figure 16 indicate that the strain at maximum stress and the ultimate strain for R1 exceeded those recorded for N1. This difference may be attributed to the increased volume of mortar in TRAC, including both the pre-existing mortar adhered to the recycled aggregate and the newly incorporated mortar, compared with the mortar content in N1. Furthermore, mortar exhibits greater compressibility than aggregate [101, 102].

Poisson's ratio exhibited a direct correlation with the horizontal strain and an inverse correlation with the modulus of elasticity, as seen in Figure 18. Incorporating one or two SCMs, such as 10% SF combined with 5% FA or 5% KA, along with 0.5% STF, as outlined in Figure 18, enhanced the modulus of elasticity in the concrete mixes. This improvement reduced transverse strain, thereby decreasing Poisson's ratio [103]. The quantitative relationship between Poisson's ratio (v) and modulus of elasticity (E_c) is expressed in Eq. (10).

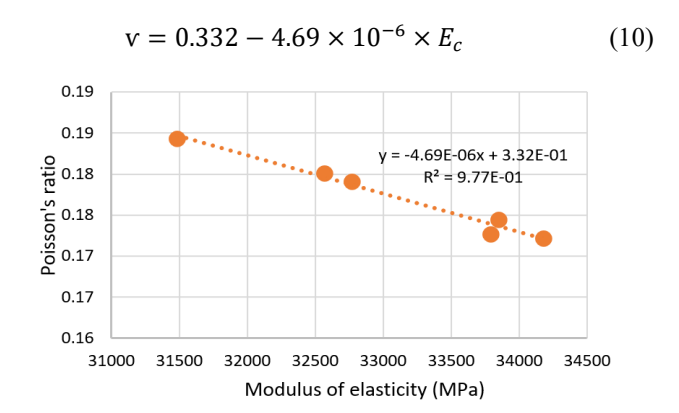


Figure 17. The correlation between Poisson's ratio and the modulus of elasticity

Incorporating one or a combination of two SCMs-10% SF,

15% FA, or 5% KA-alongside 0.5% STF in concrete mixtures led to a significant enhancement in compressive toughness, as outlined in Table 5. Concrete mixtures containing STF alone or SCMs combined with STF achieved compressive toughness values surpassing those of R1 and N1 by over 1.5 times. The use of STF in the R2-STF0.5 mixture improved the compressive toughness by 53.94% compared to R1. The

significant rise in the compressive toughness is attributed to enhanced ductility and increased vertical strain capacity, which delayed failure.

The addition of 0.5% STF in the concrete mixtures resulted in greater vertical strain and an expanded area under the stress-strain curve, substantially enhancing the compressive toughness.

Table 5. Mechanical	properties	from modul	lus of e	lasticity testing
i abic 5. Micchaillear	properties	mom mouu	us or c	lasticity testilig

Job Mixes Name	Compressive Strength σ_{cv}	Modulus of Elasticity Ec	ΔEc	Strain at Pea Stress	k Maximum Strain ε _{max}	Poisson's Ratio	Compressive Toughness CT	, ΔСΤ
	(MPa)	(MPa)	(%)	$rac{oldsymbol{arepsilon}_{oldsymbol{\sigma}_{ ext{max}}}}{(ext{-})}$	(-)	(-)	10 ⁻² × (MPa)	(%)
N1	41.62	31721	5.31	0.00185	0.00305	0.182	9.47	-9.17
R1	41.16	30122	0.00	0.00218	0.00366	0.204	10.42	0.00
R2-0.5STF	42.86	31488	4.53	0.00221	0.00585	0.184	16.05	53.94
R3-STF0.5-SF10	47.89	33851	12.38	0.00191	0.00533	0.174	16.29	56.24
R4-STF0.5-FA15	44.79	32769	8.79	0.00205	0.00582	0.179	16.55	58.73
R5-STF0.5-K5	43.90	32571	8.13	0.00200	0.00571	0.180	15.98	53.30
R6-STF0.5-SF10-FA15	5 51.60	34176	13.46	0.00183	0.00542	0.172	15.87	52.24
R7-STF0.5-SF10-K5	49.44	33792	12.18	0.00193	0.00557	0.173	15.99	53.37

3.8 Flexural strength of concrete beam using third point-loading

Three concrete beam samples were tested to determine the concrete's flexural strength and other variables. The load and corresponding deflection values were recorded to establish and analyze their correlation. Figure 19 illustrates the load-deflection curve for the eight concrete mixes. Figure 20 and Table 6 display the test results for flexural strength, deflection at the first crack, maximum deflection, flexural toughness at deflection L/150 (2 mm), and flexural stiffness.

The flexural strength of N1 was measured at 6.01 MPa, while R1 recorded 5.31 MPa, indicating an 11.66% reduction compared to N1. The decrease in the flexural strength for R1 was minimal, attributed to the treatment process of the RA used in TRAC [16]. The flexural strength results of N1 and R1 are consistent with previous studies [16].

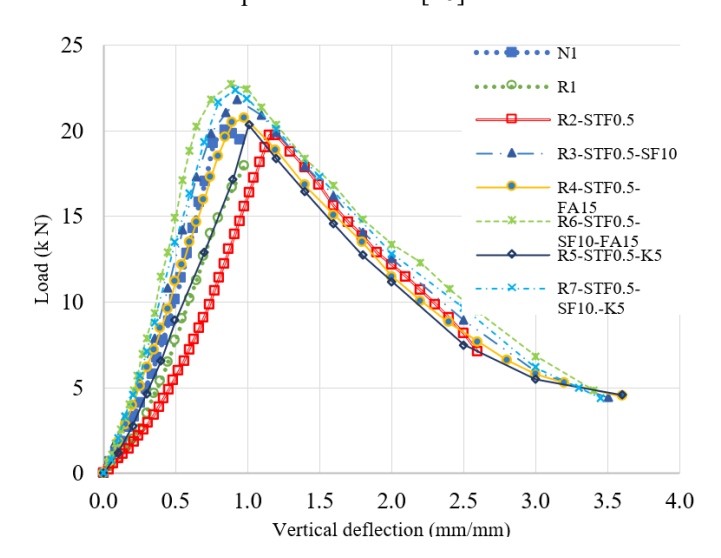


Figure 18. The correlation between the applied load and midspan deflection

Incorporating 0.5% STF into the R2-STF0.5 concrete mix resulted in a 23.8% increase in the flexural strength compared to R1, exceeding the performance of N1. This improvement is consistent with findings from previous studies on natural

aggregate concrete, providing strong evidence for the effectiveness of the RA treatment and the application of the TSMA in enhancing mechanical performance [104]. This study employed TRA in concrete, contrasting with previous studies that primarily used NA, further emphasizing the efficacy of the treatment method applied to RA [105].

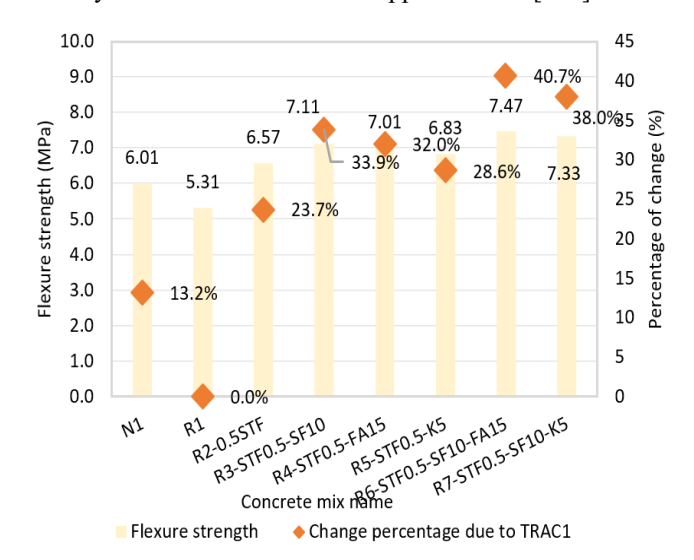


Figure 19. The flexural strength and the percentage of change of concrete mixes related to R1

Table 6. Flexural test results of concrete beams under third-point loading

Concrete Mix Name	A	В	C	D	E
	(MPa)	(mm)	(mm)	(N.m)	(N/m)
N1	6.01	0.95	0.950	9.43	24.12
R1	5.31	0.98	0.98	8.01	16.67
R2-0.5STF	6.57	0.92	4.00	25.74	25.21
R3-STF0.5-SF10	7.11	0.78	4.00	32.37	34.46
R4-STF0.5-FA15	7.01	0.81	4.00	30.71	31.66
R5-STF0.5-KA5	6.83	0.78	4.00	28.84	27.88
R6-STF0.5-SF10-FA15	7.47	0.76	4.00	34.71	38.54
R7-STF0.5-SF10-KA5	7.33	0.78	4.00	34.15	36.68

Notes: A is flexural strength; B is deflection at first crack; C is maximum deflection or the deflection at L/75; D is flexural toughness at deflection L/75; E is flexural stiffness

Adding 0.5% STF with one or two SCMs to concrete mixes significantly enhanced the flexural strength relative to R1. The flexural strength increased by 34.1%, 32.1%, and 28.8% when 0.5% STF was combined with 10% SF, 15% FA, and 5% KA, respectively, in the R3-STF0.5-SF10, R4-STF0.5-FA15, and R5-STF0.5-KA5 mixes. The findings align with previous studies, albeit for NA-based concrete [27]. The incorporation of 0.5% STF with 10% SF and either 15% FA or 5% KA in R6-STF0.5-SF10-FA15 and R7-STF0.5-SF10-KA5 further improved the flexural strength, yielding increases of 40.79% and 38.11%, respectively. Prior studies combining TRA with STF, SF, and FA were rare.

The enhancement in flexural strength is attributed to two primary factors. First, STF withstands internal tension and inhibits crack propagation, significantly improving flexural strength [79, 106]. Second, SCMs react with CH to form CSH, which enhances the compressive, tensile, and flexural strength of concrete [35]. Consequently, this combination results in a significant improvement in flexural strength.

The flexural strength test results, including mid-span deflection and applied load, were graphically represented with beam deflection on the X-axis and applied load on the Y-axis, extending deflection to L/75 (4 mm). Table 6 comprehensively presents the load-deflection test outcomes for different concrete mixtures.

The deflection at the first crack and the maximum deflection for N1 measured 0.95 mm, exhibiting brittle behavior. Incorporating 0.5% STF into R2-STF0.5 modified the beam's behavior to ductile, with the deflection at first crack of 0.92 mm and maximum deflection exceeding 4 mm. Adding one or two SCMs, specifically 10% SF, 15% FA, or 5% KA, along with 0.5% STF in R3-STF0.5-SF10, R4-STF0.5-FA15, R5-STF0.5-KA5, R6-STF0.5-SF10-FA15, and R7-STF0.5-SF10-KA5 reduced the deflection at first crack and the maximum deflection remained above 4 mm.

Figure 21 illustrates the correlation between the square root of cylindrical compressive strength and flexural strength for concrete mixtures containing 0.5% STF. This relationship follows a linear trend, as described by Eq. (11), which corresponds with the flexural strength equation outlined in ACI 363, but for natural aggregate concrete [98].

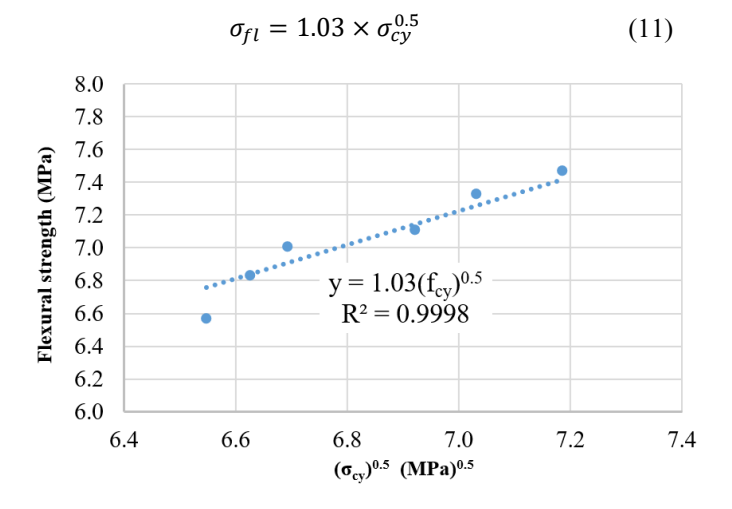


Figure 20. The correlation between the square root of cylindrical compressive strength (σ_{cy}) and the flexural strength (σ_{fl}) for STF concrete mixes

The flexural toughness, defined as the area under the loaddeflection curve, is illustrated in Table 6 and Figure 22. The flexural toughness of N1 and R1 was 9.43 N.m and 8.01 N.m, with flexural toughness of R1 being 15.05% lower than N1. Adding 0.5% STF to R2-STF0.5 significantly enhanced flexural toughness by 221.5% at 2 mm deflection, compared to R1.

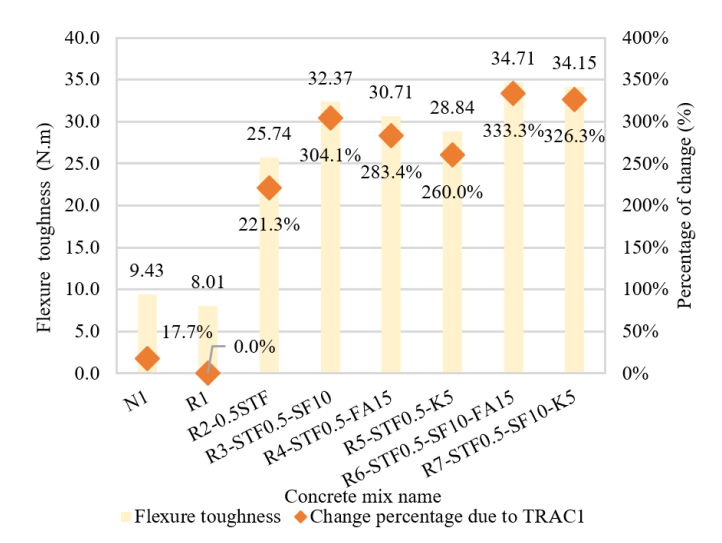


Figure 21. Flexural toughness of concrete mixes and percentage change relative to R1

The main factor contributing to the increase in flexural toughness was the higher total deflection and maximum flexural load compared to R1, demonstrating that the incorporation of 0.5% STF improved the ductility of R2-STF0.5 [107]. The current study's findings align with previous research, which primarily used natural aggregate [108].

Adding 0.5% STF with one or two SCMs, such as 10% SF, 15% FA, and 5% KA, in R3-STF0.5-SF10, R4-STF0.5-FA15, R5-STF0.5-KA5, R6-STF0.5-SF10-FA15, and R7-STF0.5-SF10-KA5 enhanced the flexural toughness by 304.33%, 283.61%, 260.18%, 333.55%, and 326.59%, respectively, at L/150 deflection, compared to R1.

The increase in flexural toughness is attributed to the incorporation of STF and SCMs. SCMs improve flexural load capacity, while STF increase both the flexural load and maximum deflection, enlarging the area under the load-deflection curve, which leads to an increase in flexural toughness [109]. The increase in flexural toughness for concrete mix R3-STF0.5-SF10 was similar to that in the previous study, but with natural aggregate [110].

The flexural stiffness values for N1, R1, and R2-STF0.5 were 24.12 N/m, 16.67 N/m, and 25.21 N/m, respectively. Incorporating SCMs with 0.5% STF enhanced the flexural stiffness by 106.78%, 90.00%, 67.29%, 131.29%, and 120.12% for R3-STF0.5-SF10, R4-STF0.5-FA15, R5-STF0.5-KA5, R6-STF0.5-SF10-FA15, and R7-STF0.5-SF10-KA5, respectively, compared to R1.

A significant increase in flexural stiffness was observed with the combination of 10% SF, 15% FA, and 0.5% STF.

3.9 Flexural impact energy and toughness

Three concrete beam samples measuring $100 \times 100 \times 500$ mm were subjected to flexural impact energy testing.

Table 7 presents the number of blows required to initiate the first crack (NB_{fcr}) , the number of blows leading to failure (NB_{fai}) , the energy needed to create the first crack (FIE_{fcr}) , the energy needed to induce failure (FIE_{fai}) and the

percentage variation of these variables relative to the R1 concrete mix.

Table 7. Illustrate the result date for the impact load test for concrete beams

Job mixes name	NB _{fcr} (blow)	NB _{fai} (blow)	FIE _{fcr} (J)	FIE _{fai} (J)	Δ _{fcr} (%)	Δ _{fai} (%)
N1	3.0	3.7	24.1	29.4	12.6	10.1
R1	2.7	3.3	21.4	26.7	0.0	0.0
R2-0.5STF	10.7	16.7	85.5	133.6	299.7	400.5
R3-STF0.5-SF10	14.3	21.3	114.9	171.0	436.8	540.5
R4-STF0.5-FA15	13.6	20.3	109.6	163.0	412.1	510.4
R5-STF0.5-KA5	13.7	18.3	109.5	147.0	411.7	450.4
R6-STF0.5-SF10-FA15	16.0	23.3	128.3	187.0	499.4	600.5
R7-STF0.5-SF10-KA5	15.3	22.7	122.9	181.7	474.3	580.7

The N1 and R1 concrete mixes exhibited first crack impact energies of 24.1 J and 21.4 J, and failure impact energies of 29.4 J and 26.7 J, respectively. Both N1 and R1 demonstrated lower impact energy resistance than STF-reinforced concrete, due to the brittle nature of both mixes.

Introducing 0.5% STF into the R2-STF0.5 concrete mix delayed the development of the first crack and ultimate failure in beam samples during the flexural impact energy test. Furthermore, the energy required for the first crack increased significantly by 299.7%, while the total energy at failure increased by 400.5%, compared to R1.

Noaman et al. [60] reported that incorporating 0.5% STF (relative to the total volume of concrete) resulted in a substantial increase in flexural impact energy. Specifically, the first-crack impact energy increased by 267.0%, while the total-failure impact energy improved by 341.4%.

Adding 0.5% STF with 10% SF, 15% FA, or 5% KA increased the first crack impact energy by 436.8%, 412.1%, and 411.7%, respectively, compared to R1. Furthermore, the failure impact energy increased by 540.5%, 510.4%, and 450.4%, respectively, compared to R1.

The integration of two SCMs with 0.5% STF in the R-STF0.5-SF10-FA15 and R7-STF0.5-SF10-KA5 concrete mixes further enhanced the first crack impact energy by 499.4% and 474.3%, respectively, relative to R1. The failure impact energy also improved, showing increases of 600.5% and 580.7%, respectively, compared to R1.

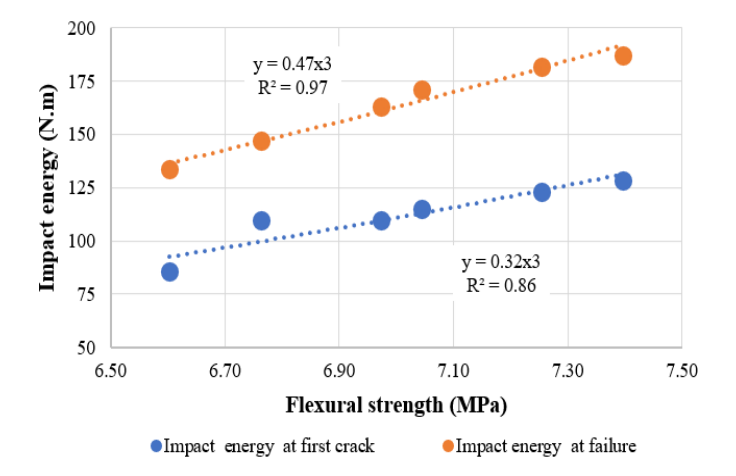


Figure 22. Relationship between flexural strength and impact energy at first crack and failure in STF-reinforced concrete

Figure 23 illustrates a positive correlation between static

flexural strength and flexural impact energy, as described by Eq. (12) and Eq. (13). These formulas indicate that the failure impact energy is 1.47 times greater than the energy required to initiate the first crack in concrete containing STF.

$$FIE_{fcr} = 0.32 \times \sigma_{fl}^3 \text{ First crack}$$
 (12)

$$FIE_{fai} = 0.47 \times \sigma_{fl}^3 \text{ Failure}$$
 (13)

4. CONCLUSION

This study demonstrated that replacing 100% natural aggregate with treated recycled aggregate (TRA) in concrete, combined with the two-stage mixing approach (TSMA) and the incorporation of 0.5% steel fibers (STF) and supplementary cementitious materials (SCMs), significantly enhanced the concrete's mechanical properties, durability, and impact resistance.

The inclusion of SCMs (10% SF, 15% FA, or 5% KA), either individually or in combination with STF, improved the compressive, splitting tensile, flexural strength, and modulus of elasticity while reducing absorption, porosity, and permeability. The most notable strength enhancement was observed in R3-STF0.5-SF10, which exhibited increases of 18.97% in compressive strength, 32.77% in splitting tensile strength, 34.1% in flexural strength, and 12.38% in modulus of elasticity. Additionally, durability parameters improved significantly, with absorption and porosity reduced by 32.9% and 32.8%, while rapid chloride permeability and water permeability decreased by 76.5% and 74.7%, respectively.

A combination of 10% SF, 15% FA, and 0.5% STF (R6-STF0.5-SF10-FA15) further enhanced concrete performance, achieving increases of 28.92% in compressive strength, 38.62% in splitting tensile strength, 40.80% in flexural strength, and 13.46% in modulus of elasticity. The R6-STF0.5-SF10-FA15 mix exhibited superior durability compared to conventional and RAC, with reductions of 38.2% in absorption, 37.90% in porosity, 81.50% in water permeability, and 84.4% in rapid chloride permeability.

Incorporating 0.5% STF, alone or with SCMs, significantly improved flexural toughness and stiffness. The R3-STF0.5-SF10 mix enhanced flexural toughness by over 300% and FLST stiffness by over 100%. The highest enhancement was observed in R6-STF0.5-SF10-FA15, where flexural toughness increased by over 330% and FLST stiffness by over 130% compared to R1. The inclusion of STF and SCMs also enhanced FIE, with R2-STF0.5 achieving 300% and 400% increases at first crack and failure, respectively. R6-STF0.5-SF10-FA15 exhibited the highest impact resistance, with 500% and 600% improvements at first crack and failure, respectively.

Overall, treating recycled aggregate with 0.1M HCl, employing TSMA, and incorporating STF and SCMs significantly enhanced the performance of RAC. The optimized mixtures outperformed conventional concrete in terms of strength, durability, ductility, and resistance to dynamic loads, with silica fume proving to be the most effective SCM for enhancing these properties. Incorporating STF and SCMs significantly improves concrete's mechanical and durability performance, making it a promising material for demanding engineering applications such as bridge decks, pavements, and precast elements exposed to harsh environments and high impact loads.

5. LIMITATIONS AND FUTURE WORK

This study primarily focused on short-term mechanical performance, offering valuable insights into the early-age behavior of the proposed concrete. To extend these findings, future research should evaluate its long-term durability under aggressive environments. In particular, durability assessments involving freeze-thaw cycling (ASTM C666) and sulphate exposure (ASTM C1012) are recommended to determine resistance to scaling, microcracking, dimensional stability, and chemical degradation. Such investigations will provide a more comprehensive understanding of the material's service life and strengthen its suitability for critical infrastructure applications.

ACKNOWLEDGEMENT

The authors gratefully acknowledge Universiti Sains Malaysia for providing the raw materials for this research. This study is funded under Short Term Grant (R501-LR-RND002-0000001037-0000). Additionally, the author acknowledges with appreciation the partial support received from the Palestinian American Research Center (PARC).

AUTHOR CONTRIBUTION

The authors confirm contribution to the paper as follows: Data Curation, Writing - Original Draft Preparation, Investigation: Bassam Suliman Dabbour; Writing - Reviewing and Editing: Mohd Zulham Affandi Bin Mohd Zahid; Methodology and Supervision: Badorul Hisham Bin Abu Bakar; Investigation: Noorhazlinda Binti Abd Rahman, Abrahem Ahsin Blash.

REFERENCES

- [1] Islam, N., Sandanayake, M., Muthukumaran, S., Navaratna, D. (2024). Review on sustainable construction and demolition waste management-Challenges and research prospects. Sustainability, 16(8): 3289. https://doi.org/10.3390/su16083289
- [2] Tam, V.W.Y., Soomro, M., Evangelista, A.C.J. (2018). A review of recycled aggregate in concrete applications (2000-2017). Construction and Building Materials, 172: 272-292. https://doi.org/10.1016/j.conbuildmat.2018.03.240
- [3] Zhang, J., Ding, L., Li, F., Peng, J. (2020). Recycled aggregates from construction and demolition wastes as alternative filling materials for highway subgrades in China. Journal of Cleaner Production, 255: 120223. https://doi.org/10.1016/j.jclepro.2020.120223
- [4] Wagih, A.M., El-Karmoty, H.Z., Ebid, M., Okba, S.H. (2013). Recycled construction and demolition concrete waste as aggregate for structural concrete. HBRC Journal, 9(3): 193-200. https://doi.org/10.1016/j.hbrcj.2013.08.007
- [5] Poon, C.S., Chan, D. (2007). The use of recycled aggregate in concrete in Hong Kong. Resources, Conservation and Recycling, 50(3): 293-305. https://doi.org/10.1016/j.resconrec.2006.06.005
- [6] Sasanipour, H., Aslani, F., Taherinezhad, J. (2021).

- Chloride ion permeability improvement of recycled aggregate concrete using pretreated recycled aggregates by silica fume slurry. Construction and Building Materials, 270: 121498. https://doi.org/10.1016/j.conbuildmat.2020.121498
- [7] Wang, B., Yan, L., Fu, Q., Kasal, B. (2021). A comprehensive review on recycled aggregate and recycled aggregate concrete. Resources, Conservation and Recycling: 171, 105565. https://doi.org/10.1016/j.resconrec.2021.105565
- [8] Tanta, A., Kanoungo, A., Singh, S., Kanoungo, S. (2021). The effects of surface treatment methods on properties of recycled concrete aggregates. Materials Today: Proceedings, 50: 1848-1852. https://doi.org/10.1016/j.matpr.2021.09.223
- [9] Ataria, R.B., Wang, Y.C. (2023). Improving the mechanical properties of recycled aggregate concrete with graphene. European Journal of Environmental and Civil Engineering, 27(4): 1747-1762. https://doi.org/10.1080/19648189.2022.2095034
- [10] Bai, G., Zhu, C., Liu, C., Liu, B. (2020). An evaluation of the recycled aggregate characteristics and the recycled aggregate concrete mechanical properties. Construction and Building Materials, 241: 117978. https://doi.org/10.1016/j.conbuildmat.2019.117978
- [11] Joseph, H.S., Pachiappan, T., Avudaiappan, S., Flores, E.I.S. (2022). A study on mechanical and microstructural characteristics of concrete using recycled aggregate. Materials, 15(21): 7535. https://doi.org/10.3390/ma15217535
- [12] Nachimuthu, B., Viswanathan, R., Subramaniyan, Y., Baskaran, J. (2024). Mechanical properties of recycled concrete aggregates with superplasticizer. Matéria (Rio de Janeiro), 29: e20230382. https://doi.org/10.1590/1517-7076-rmat-2023-0382
- [13] Alqarni, A.S., Abbas, H., Al-Shwikh, K.M., Al-Salloum, Y.A. (2021). Treatment of recycled concrete aggregate to enhance concrete performance. Construction and Building Materials, 307: 124960. https://doi.org/10.1016/j.conbuildmat.2021.124960
- [14] Mujaheed, Y., Xiaoshan, Z., Peiqiang, C., Xiaowu, T. (2022). Durability of recycled concrete aggregate prepared with mechanochemical and thermal treatment. Materials, 15: 5792
- [15] Saravanakumar, P., Manoj, D., Jagan, S. (2021). Properties of concrete having treated recycled coarse aggregate and slag. Revista de la Construcción, 20(2): 249-258. https://doi.org/10.7764/RDLC.20.2.249
- [16] Raman, V.M., Ramasamy, V. (2023). Dissimilar surface treated recycled coarse aggregate in concrete. Cement Lime Concrete, 28: 146-168. https://doi.org/10.32047/CWB.2023.28.3.2
- [17] Madhavarao, G.D.R., Dheeraz, V.T.S., Ramya, T., Mahesh, T., Vasu, B.B. (2023). Evaluating the performance of acid-treated (HCl-HNO₃) recycled aggregate in environmentally friendly concrete. International Journal of Innovative Research in Engineering Management, 10(2): 99-102. https://doi.org/10.55524/ijirem.2023.10.2.18
- [18] Raman, J.V.M., Ramasamy, V. (2021). Various treatment techniques involved to enhance the recycled coarse aggregate in concrete: A review. Materials Today: Proceedings, 45: 6356-6363. https://doi.org/10.1016/j.matpr.2020.10.935

- [19] Savva, P., Ioannou, S., Oikonomopoulou, K., Nicolaides, D., Petrou, M.F. (2021). A mechanical treatment method for recycled aggregates and its effect on recycled aggregate-based concrete. Materials, 14(9): 2186. https://doi.org/10.3390/ma14092186
- [20] Alqarni, A.S., Abbas, H., Al-Shwikh, K.M., Al-Salloum, Y.A. (2022). Influence of treatment methods of recycled concrete aggregate on behavior of high-strength concrete. Buildings, 12(4): 494. https://doi.org/10.3390/buildings12040494
- [21] Kansal, M.C., Goyal, R. (2021). Analysing mechanical properties of concrete with nano silica, silica fume and steel slag. Materials Today: Proceedings, 45: 4520-4525.
- [22] Sahoo, S., Parhi, K.P., Panda, G.B. (2021). Durability properties of concrete with silica fume and husk ash. Materials Today: Proceedings, 48: 1789-1795. https://doi.org/10.1016/j.matpr.2021.08.347
- [23] Khamees, A.A., Jawad, R.R., Al-Rammahi, A.A. (2024). Performance evaluation of reactive powder concrete structural members based on experimental and numerical analysis: A review. Revue des Composites et des Matériaux Avancés, 34(6): 807-814. https://doi.org/10.18280/rcma.340615
- [24] Arshad, M.T., Ahmad, S., Khitab, A., Hanif, A. (2021). Synergistic use of fly ash and silica fume to produce high-strength self-compacting cementitious composites. Crystals, 11(8): 915. https://doi.org/10.3390/cryst11080915
- [25] Zaini, M.S.I., Hasan, M., Almuaythir, S., Hyodo, M. (2024). Experimental investigations on physico-mechanical properties of kaolinite clay soil stabilized at optimum silica fume content using clamshell ash and lime. Scientific Reports, 14: 61854. https://doi.org/10.1038/s41598-024-61854-1
- [26] Nochaiya, T., Wongkeo, W., Chaipanich, A. (2010). Utilization of fly ash with silica fume and properties of Portland cement-fly ash-silica fume concrete. Fuel, 89(3): 768-774. https://doi.org/10.1016/j.fuel.2009.10.003
- [27] Nagrockiene, D., Rutkauskas, A., Pundiene, I., Girniene, I. (2019). The effect of silica fume addition on the resistance of concrete to alkali-silica reaction. Materials Science and Engineering, 660(1): 012031. https://doi.org/10.1088/1757-899X/660/1/012031
- [28] Ahmed, A. (2024). Assessing the effects of supplementary cementitious materials on concrete properties: A review. Discover Civil Engineering, 1(1): 145. https://doi.org/10.1007/s44290-024-00154-z
- [29] Yaseen, N., Alcivar-Bastidas, S., Irfan-ul-Hassan, M., Petroche, D.M., Qazi, A.U., Ramirez, A.D. (2024). Concrete incorporating supplementary cementitious materials: Temporal evolution of compressive strength and environmental life cycle assessment. Heliyon, 10(3): e25056. https://doi.org/10.1016/j.heliyon.2024.e25056
- [30] Papadakis, V.G. (1999). Experimental investigation and theoretical modeling of silica fume activity in concrete. Cement and Concrete Research, 29(1): 79-86. https://doi.org/10.1016/S0008-8846(98)00171-9
- [31] ACI Committee 318. (2019). Building code requirements for structural concrete (ACI 318-19) and commentary (ACI 318R-19). American Concrete Institute.
- [32] Kurda, R., de Brito, J., Silvestre, J.D. (2017). Combined influence of recycled concrete aggregates and high

- contents of fly ash on concrete properties. Construction and Building Materials, 157: 141-152. https://doi.org/10.1016/j.conbuildmat.2017.09.128
- [33] Abu Bakar, A., Noaman, A.T., Akil, H.M. (2017). Cumulative effect of crumb rubber and steel fiber on the flexural toughness of concrete. Engineering, Technology Applied Science Research, 7(5): 2026-2031. Retrieved from http://www.etasr.com
- [34] Koo, D.H., Kim, J.S., Kim, S.H., Suh, S.W. (2023). Evaluation of flexural toughness of concrete reinforced with high-performance steel fiber. Materials, 16(20): 6623. https://doi.org/10.3390/ma16206623
- [35] Kumar, M.H., Saikrishnamacharyulu, I., Mohanta, N.R., Ashutosh, A., Mishra, P., Samantaray, S. (2022). Mechanical behaviour of high strength concrete modified with triple blend of fly ash, silica fume and steel fibers. Materials Today: Proceedings, 65: 933-942. https://doi.org/10.1016/j.matpr.2022.03.528
- [36] Lisantono, A., Pratama, Y.P.B. (2020). Effect of silica fume on the compressive strength and modulus elasticity of self-compacting high strength concrete. IOP Conference Series: Earth and Environmental Science, 426(1): 012057. https://doi.org/10.1088/1755-1315/426/1/012057
- [37] Jagan, S., Neelakantan, R.T. (2021). Effect of silica fume on the hardened and durability properties of concrete. International Review of Applied Sciences and Engineering, 12(1): 44-49. https://doi.org/10.1556/1848.2021.00107
- [38] Sahoo, S., Parhi, P.K., Panda, B.C. (2021). Durability properties of concrete with silica fume and rice husk ash. Clean Engineering and Technology, 2: 100067. https://doi.org/10.1016/j.clet.2021.100067
- [39] Kumar, S., Rai, B. (2022). Synergetic effect of fly ash and silica fume on the performance of high-volume fly ash self-compacting concrete. Journal of Structural Integrity and Maintenance, 7(1): 61-74. https://doi.org/10.1080/24705314.2021.1892571
- [40] Kararas, M., Benli, A., Arslan, F. (2020). The effects of kaolin and calcined kaolin on the durability and mechanical properties of self-compacting mortars subjected to high temperatures. Construction and Building Materials, 265: 120761. https://doi.org/10.1016/j.conbuildmat.2020.120761
- [41] Arslan, F., Benli, A., Karatas, M. (2020). Effect of high temperature on the performance of self-compacting mortars produced with calcined kaolin and metakaolin. Construction and Building Materials, 256: 119497. https://doi.org/10.1016/j.conbuildmat.2020.119497
- [42] Laxmi, G., Patil, S., Hossiney, N., Thejas, H.K. (2023). Effect of hooked end steel fibers on strength and durability properties of ambient cured geopolymer concrete. Case Studies in Construction Materials, 18: e02122. https://doi.org/10.1016/j.cscm.2023.e02122
- [43] Udi, U.J., Almeshal, I., Johari, M.A.M., Zahid, M.M., et al. (2022). Efficiency of high performance fiber reinforced cementitious composites as a retrofit material for fire-damaged concrete. Materials Today: Proceedings, 61: 477-486. https://doi.org/10.1016/j.matpr.2021.12.278
- [44] Ashkezari, G.D., Fotouhi, F., Razmara, M. (2020). Experimental relationships between steel fiber volume fraction and mechanical properties of ultra-high performance fiber-reinforced concrete. Journal of

- Building Engineering, 32: 101613. https://doi.org/10.1016/j.jobe.2020.101613
- [45] Mujalli, M.A., Dirar, S., Mushtaha, E., Hussien, A., Maksoud, A. (2022). Evaluation of the tensile characteristics and bond behaviour of steel fibrereinforced concrete: An overview. Fibers, 10(12): 104. https://doi.org/10.3390/fib10120104
- [46] Shaban, A.M., Zeyad, A.M., Alabi, S.A., Alharbi, Y.R. (2025). Enhancing the strength and durability of sustainable concrete: The impact of recycled concrete aggregate and glass powder. Civil Engineering Journal, 11(09): 2304-2323. https://doi.org/10.28991/CEJ-2025-011-09-023
- [47] Tam, V.W.Y., Tam, C.M. (2008). Diversifying two-stage mixing approach (TSMA) for recycled aggregate concrete: TSMAs and TSMAsc. Construction and Building Materials, 22(10): 2068-2077. https://doi.org/10.1016/j.conbuildmat.2007.07.024
- [48] ASTM International. (2022). Standard Test Method for Density, Absorption, and Voids in Hardened Concrete (ASTM C642-21). ASTM International. https://doi.org/10.1520/C0642-21
- [49] ASTM International. (2022). Standard Test Method for Static Modulus of Elasticity and Poisson'S Ratio of Concrete in Compression (ASTM C469/C469M-22). ASTM International. https://doi.org/10.1520/C0469 C0469M-22
- [50] ASTM International. (2022). Standard Test Method for Flexural Strength of Concrete (Using Simple Beam with Third-point Loading) (ASTM C78/C78M-22). ASTM International. https://doi.org/10.1520/C0078_C0078M-22
- [51] ASTM International. (2022). Standard Test Method for Electrical Indication of Concrete's Ability to Resist Chloride Ion Penetration (ASTM C1202-22). ASTM International. https://doi.org/10.1520/C1202-22
- [52] ASTM International. (2020). Standard Test Method for Slump of Hydraulic-cement Concrete (ASTM C143/C143M-20). ASTM International. https://doi.org/10.1520/C0143 C0143M-20
- [53] ASTM International. (2020). Standard Practice for Making and Curing Concrete Test Specimens in the Laboratory (ASTM C192/C192M-19). ASTM International. https://doi.org/10.1520/C0192_C0192M-19
- [54] American Concrete Institute (ACI). (1991). Standard Practice for Selecting Proportions for Normal, Heavyweight, and Mass Concrete (ACI 211.1-91). Reported by ACI Committee 211, Chairman, Subcommittee A. Farmington Hills, MI: American Concrete Institute
- [55] Hedegaard, S.E., Hansen, T.C. (1992). Water permeability of fly ash concretes. Materials and Structures, 25: 381-387. https://doi.org/10.1007/BF02472253
- [56] ASTM International. (2022). Standard Test Method for Electrical Indication of Concrete'S Ability to Resist Chloride Ion Penetration (ASTM C1202-22). ASTM International. https://doi.org/10.1520/C1202-22
- [57] British Standards Institution. (2019). BS EN 12390-3:2019. Testing hardened concrete Part 3: Compressive strength of test specimens. BSI Standards.
- [58] ASTM International. (2017). Standard Test Method for Splitting Tensile Strength of Cylindrical Concrete

- Specimens (ASTM C496/C496M-17). ASTM International. https://doi.org/10.1520/C0496_C0496M-17
- [59] ASTM International. (2007). Standard Test Method for Flexural Performance of Fiber-reinforced Concrete (using beam with third-point loading) (ASTM C1609/C1609M-07). ASTM International. Retrieved from https://www.astm.org
- [60] Noaman, A.T., Bakar, B.H.A., Akil, H. (2015). The effect of combination between crumb rubber and steel fiber on impact energy of concrete beams. Procedia Engineering, 125: 825-831. https://doi.org/10.1016/j.proeng.2015.11.148
- [61] Hao, Y., Hao, H., Chen, G. (2016). Experimental investigation of the behaviour of spiral steel fibre reinforced concrete beams subjected to drop-weight impact loads. Materials and Structures, 49(1-2): 353-370. https://doi.org/10.1617/s11527-014-0502-5
- [62] Al Ajmani, H., Suleiman, F., Abuzayed, I., Tamimi, A. (2019). Evaluation of concrete strength made with recycled aggregate. Buildings, 9(3): 56. https://doi.org/10.3390/buildings9030056
- [63] Verian, K.P., Ashraf, W., Cao, Y. (2018). Properties of recycled concrete aggregate and their influence in new concrete production. Resources, Conservation and Recycling, 133: 30-49. https://doi.org/10.1016/j.resconrec.2018.02.005
- [64] Cartuxo, F., De Brito, J., Evangelista, L., Jiménez, J.R., Ledesma, E.F. (2016). Increased durability of concrete made with fine recycled concrete aggregates using superplasticizers. Materials, 9(2): 98. https://doi.org/10.3390/ma9020098
- [65] Tam, Y., Gao, X.F., Tam, C.M. (2006). Comparing performance of modified two-stage mixing approach for producing recycled aggregate concrete. Magazine of Concrete Research, 58(7): 477-484. https://doi.org/10.1680/macr.2006.58.7.477
- [66] Uniyal, S., Aggrawal, V. (2014). Comparison of compressive strength of concrete made by two-stage mixing approach (TSMA) using fly ash and nominal concrete made by normal mixing approach (NMA). International Journal of Engineering Research Technology, 3(7): 299-302.
- [67] Ahmad, J., Zhou, Z., Deifalla, A.F. (2023). Steel fiber reinforced self-compacting concrete: A comprehensive review. International Journal of Concrete Structures and Materials, 17(1): 1-21. https://doi.org/10.1186/s40069-023-00602-7
- [68] Köksal, F., Altun, F., Yiğit, I., Şahin, Y. (2008). Combined effect of silica fume and steel fiber on the mechanical properties of high strength concretes. Construction and Building Materials, 22(8): 1874-1880. https://doi.org/10.1016/j.conbuildmat.2007.04.017
- [69] Ahmed, A. (2024). Assessing the effects of supplementary cementitious materials on concrete properties: A review. Discover Civil Engineering, 1(1): 145. https://doi.org/10.1007/s44290-024-00154-z
- [70] Güneyisi, E., Gesoğlu, M., Karaoğlu, S., Mermerdaş, K. (2012). Strength, permeability and shrinkage cracking of silica fume and metakaolin concretes. Construction and Building Materials, 34: 120-130. https://doi.org/10.1016/j.conbuildmat.2012.02.017
- [71] Lin, W.T., Huang, R., Chang, J.J., Lee, C.L. (2009). Effect of silica fumes on the permeability of fiber cement

- composites. Journal of the Chinese Institute of Engineers, 32(4): 531-541. https://doi.org/10.1080/02533839.2009.9671535
- [72] Miloud, B. (2008). Permeability and porosity as an essential factors in the long-term durability of steel fibres reinforced concrete. In Proceedings of the 11th International Conference on Durability of Building Materials and Components, Istanbul, Turkey, pp. 11-14.
- [73] Tan, Y., Xu, Z., Liu, Z., Jiang, J. (2022). Effect of silica fume and polyvinyl alcohol fiber on mechanical properties and frost resistance of concrete. Buildings, 12(1): 47. https://doi.org/10.3390/buildings12010047
- [74] Ahmed, A. (2024). Assessing the effects of supplementary cementitious materials on concrete properties: A review. Discover Civil Engineering, 1(1): 145. https://doi.org/10.1007/s44290-024-00154-z
- [75] Kumar, V.P., Prasad, D.R. (2019). Influence of supplementary cementitious materials on strength and durability characteristics of concrete. Advances in Concrete Construction, 7(2): 75. https://doi.org/10.12989/acc.2019.7.2.075
- [76] Yunchao, T., Zheng, C., Wanhui, F., Yumei, N., Cong, L., Jieming, C. (2021). Combined effects of nano-silica and silica fume on the mechanical behavior of recycled aggregate concrete. Nanotechnology Reviews, 10(1): 819-838. https://doi.org/10.1515/ntrev-2021-0058
- [77] Qureshi, L.A., Ali, B., Ali, A. (2020). Combined effects of supplementary cementitious materials (silica fume, GGBS, fly ash and rice husk ash) and steel fiber on the hardened properties of recycled aggregate concrete. Construction and Building Materials, 263: 120636. https://doi.org/10.1016/j.conbuildmat.2020.120636
- [78] Lin, W.T., Huang, R., Chang, J.J., Lee, C.L. (2009). Effect of silica fumes on the permeability of fiber cement composites. Journal of the Chinese Institute of Engineers, 32(4): 531-541. https://doi.org/10.1080/02533839.2009.9671535
- [79] Akhtar, T., Ali, B., Kahla, N.B., Kurda, R., et al. (2022). Experimental investigation of eco-friendly high strength fiber-reinforced concrete developed with combined incorporation of tyre-steel fiber and fly ash. Construction and Building Materials, 314: 125626. https://doi.org/10.1016/j.conbuildmat.2021.125626
- [80] Huang, K.S., Yang, C.C. (2018). Using RCPT to determine the migration coefficient to assess the durability of concrete. Construction and Building Materials, 167: 822-830. https://doi.org/10.1016/j.conbuildmat.2018.02.109
- [81] Yodsudjai, W., Nitichote, K. (2022). Chloride penetration behavior of concrete made from various types of recycled concrete aggregate. Sustainability, 14(5): 2768. https://doi.org/10.3390/su14052768
- [82] Macmac, J.D., Clemente, S.J.C., Ongpeng, J.M.C. (2024). Corrosion resistance analysis of tire waste steel fiber reinforced self-compacting concrete using rapid chloride penetration test. Chemical Engineering Transactions, 114: 463-468. https://doi.org/10.3303/CET24114078
- [83] Shafiq, N., Kumar, R., Zahid, M., Tufail, R.F. (2019). Effects of modified metakaolin using nano-silica on the mechanical properties and durability of concrete. Materials, 12(14): 2291. https://doi.org/10.3390/ma12142291
- [84] Kumar, C.P., Anandhi, L. (2022). Experimental

- investigation on partial replacement of cement with Metakaoline, fly ash and silica fume in concrete. Sustainable Materials and Smart Practices: NCSMSP-2021, 23: 50. https://doi.org/10.21741/9781644901953-7
- [85] Abdo, A., El-Zohairy, A., Alashker, Y., Badran, M.A.E.A., Ahmed, S. (2024). Effect of treated/untreated recycled aggregate concrete: Structural behavior of RC beams. Sustainability, 16(10): 4039. https://doi.org/10.3390/su16104039
- [86] Qureshi, L.A., Ali, B., Ali, A. (2020). Combined effects of supplementary cementitious materials (silica fume, GGBS, fly ash and rice husk ash) and steel fiber on the hardened properties of recycled aggregate concrete. Construction and Building Materials, 263: 120636. https://doi.org/10.1016/j.conbuildmat.2020.120636
- [87] Zhang, P., Wang, C., Gao, Z., Wang, F. (2023). A review on fracture properties of steel fiber reinforced concrete. Journal of Building Engineering, 67: 105975. https://doi.org/10.1016/j.jobe.2023.105975
- [88] Ali, B., Ahmed, H., Ali Qureshi, L., Kurda, R., Hafez, H., Mohammed, H., Raza, A. (2020). Enhancing the hardened properties of recycled concrete (RC) through synergistic incorporation of fiber reinforcement and silica fume. Materials, 13(18): 4112. https://doi.org/10.3390/ma13184112
- [89] Ren, G.M., Wu, H., Fang, Q., Liu, J.Z. (2018). Effects of steel fiber content and type on static mechanical properties of UHPCC. Construction and Building Materials, 163: 826-839. https://doi.org/10.1016/j.conbuildmat.2017.12.184
- [90] Khan, M., Ali, M. (2019). Improvement in concrete behavior with fly ash, silica-fume and coconut fibres. Construction and Building Materials, 203: 174-187. https://doi.org/10.1016/j.conbuildmat.2019.01.103
- [91] Perumal, R. (2015). Correlation of compressive strength and other engineering properties of high-performance steel fiber-reinforced concrete. Journal of Materials in Civil Engineering, 27(1): 04014111. https://doi.org/10.1061/(ASCE)MT.1943-5533.0001050
- [92] Bickley, J.A., Aïtcin, P.C., Iravani, S., Russell, H.G., et al. (1998). Guide to quality control and testing of high-strength concrete.
- [93] Xu, B.W., Shi, H.S. (2009). Correlations among mechanical properties of steel fiber reinforced concrete. Construction and Building Materials, 23(12): 3468-3474.
 - https://doi.org/10.1016/j.conbuildmat.2009.08.017
- [94] Anoglu, N., Girgin, Z., Anoglu, E. (2006). Evaluation of ratio between splitting tensile strength and compressive strength for concretes up to 120 MPa and its application in strength criterion. ACI Materials Journal, 103(1): 18-24.
- [95] Sun, R.W., Fanourakis, G.C. (2022). The validation of elastic modulus models: Code models and their modified versions. Structural Concrete, 23(5): 3039-3049. https://doi.org/10.1002/suco.202100312
- [96] Chen, J., Zhou, Y., Yin, F. (2022). A practical equation for the elastic modulus of recycled aggregate concrete. Buildings, 12(2): 187. https://doi.org/10.3390/buildings12020187
- [97] Comité Euro-International du Béton (CEB). (1998). CEB-FIP model code for concrete structures 1990. London: Thomas Telford Services Ltd.

- [98] American Concrete Institute (ACI). (2011). Building code requirements for structural concrete (ACI 318-11) and commentary. Farmington Hills, MI: American Concrete Institute.
- [99] Malaikah, A.S. (2004). A proposed relationship for the modulus of elasticity of high strength concrete using local materials in Riyadh. King Saud University Journal, 17(2): 131-142. https://doi.org/10.1016/S1018-3639(18)30804-3
- [100]ACI Committee 363. (1997). State-of-the-art report on high-strength concrete. Farmington Hills, MI: American Concrete Institute.
- [101] Tariq, F., Hasan, H., Bhargava, P. (2024). Stress-strain characteristics of fire-exposed recycled coarse aggregate concrete. Structural Concrete, 25(5): 4012-4032. https://doi.org/10.1002/suco.202301060
- [102] Yang, A., Shang, Q., Zhang, Y., Zhu, J. (2024). Research on macroscopic mechanical behavior of recycled aggregate concrete based on mesoscale. Materials, 17(11): 2532. https://doi.org/10.3390/ma17112532
- [103]Zende, A.A., Momin, A.I.A., Khadiranaikar, R.B., Alsabhan, A.H., et al. (2023). Mechanical properties of high-strength self-compacting concrete. ACS Omega, 8(20): 18000-18008. https://doi.org/10.1021/acsomega.3c01204
- [104]Choi, W.C., Jung, K.Y., Jang, S.J., Yun, H.D. (2019). The influence of steel fiber tensile strengths and aspect ratios on the fracture properties of high-strength concrete. Materials, 12(13): 2105. https://doi.org/10.3390/ma12132105
- [105]Turk, K., Bassurucu, M., Bitkin, R.E. (2021). Workability, strength and flexural toughness properties of hybrid steel fiber reinforced SCC with high-volume fiber. Construction and Building Materials, 266: 120944. https://doi.org/10.1016/j.conbuildmat.2020.120944
- [106]Kumar, M.H., Saikrishnamacharyulu, I., Mohanta, N.R., Ashutosh, A., Mishra, P., Samantaray, S. (2022). Mechanical behaviour of high strength concrete modified with triple blend of fly ash, silica fume and steel fibers. Materials Today: Proceedings, 65: 933-942. https://doi.org/10.1016/j.matpr.2022.03.528
- [107] Bayraktar, O.Y., Kaplan, G., Shi, J., Benli, A., Bodur, B., Turkoglu, M. (2023). The effect of steel fiber aspect ratio and content on the fresh, flexural, and mechanical performance of concrete made with recycled fine aggregate. Construction and Building Materials, 368: 130497

https://doi.org/10.1016/j.conbuildmat.2023.130497

- [108] Wang, S., Zhu, H., Liu, F., Cheng, S., Wang, B., Yang, L. (2022). Effects of steel fibers and concrete strength on flexural toughness of ultra-high performance concrete with coarse aggregate. Case Studies in Construction Materials, 17: e01170. https://doi.org/10.1016/j.cscm.2022.e01170
- [109]Mehta, A., Ashish, D.K. (2020). Silica fume and waste glass in cement concrete production: A review. Journal of Building Engineering, 27: 100888.

https://doi.org/10.1016/j.jobe.2019.100888

[110]Zeyad, A.M. (2020). Effect of fiber types on fresh properties and flexural toughness of self-compacting concrete. Journal of Materials Research and Technology, 9(3):

4147-4158.

https://doi.org/10.1016/j.jmrt.2020.02.042

NOMENCLATURE

RA	recycled aggregate
RAC	recycled aggregate concrete
TRAC	treated recycled aggregate concrete
TMSA	two-stage mixing approach
STF	Steel fiber

SCM supplementary cementitious material SF silica fume FA fly ash

KA kaolin

NA natural aggregate

NAC natural aggregate concrete

CH calcium hydroxide

CSH calcium silicate hydrate

SG specific gravity, dimensionless

ABS water absorption, % USM Universiti Sains Malaysia

RS river sand

OPC ordinary Portland cement SEM scanning electron microscopy

 ρ density, kg/m³

n porosity, dimensionless

RCP Rapid chloride permeability, Coulombs

K water permeability, m/s

P vertical load, N

E_c modulus of elasticity, GPa CT compressive toughness, MPa

FT flexural toughness, J
FS flexural stiffness, N.m⁻¹
FIE flexural impact energy, J
NB number of blows, number

Greek symbols

σ strength, MPa
 v Poisson's ratio, dimensionless
 ε STRAIN; dimensionless
 δ beam deflection, mm

Subscripts

c cube compressive sp splitting fl flexural cy clindtical max maximum fcr first crack fai at failure